UNIVERSITY OF CALIFORNIA, SAN DIEGO

Mechanism, Function and Modulation of Oncogenic Cripto Signaling

A dissertation submitted in partial satisfaction of the requirements for

the degree of Doctor of Philosophy

in

Chemistry

by

Jonathan A. Kelber

Committee in charge:

Professor Wylie Vale, Chair
Professor Alexander Hoffmann, Co-Chair
Professor Daniel Donoghue
Professor Peter Wolynes
Professor Shunichi Shimasaki

2009

The Dissertation of Jonathan A. Kelber is approved, and it is acceptable in quality and form for publication on microfilm and electronically:

Co-Chair

Chair

University of California, San Diego

2009

DEDICATION

This body of work would not have been possible if it were not for the tremendous love and encouragement that I have received from my wife, Julie. In many ways, Julie encouraged me to attend graduate school and she has remained my most loyal supporter throughout this endeavor. We are excitedly awaiting the arrival of our first child and I am so excited to partner with Julie in this next chapter of our family's life. It is for these reasons, as well as others too numerous to mention, that I dedicate this dissertation to my loving wife Julie and our son.

TABLE OF CONTENTS

LIST OF FIGURES

Chapter 1

Chapter 2

ACKNOWLEDGEMENTS

It has been a tremendous honor to be a member of Wylie Vale's research laboratory at the Salk Institute for Biological Studies. The professionalism and scientific expertise that has been developed over the course of more than three decades of outstanding research have provided an exceptional training environment for me. I am very grateful to Wylie for accepting me into his laboratory and providing outstanding guidance and counsel throughout my graduate studies. In addition to the one-on-one guidance that he has provided, Wylie has also hired and retained outstanding scientists. Much of my success as a graduate student in the Vale Lab can be attributed, in no small part, to these individuals that I have had the opportunity to train along side. Their willingness to collaborate and offer advice has facilitated my progress greatly. I would like to thank the following members for their expertise in the molecular and cell biology/biochemistry of TGF-β signaling: Louise Bilezikjian, Woflgang Fischer, Gidi Shani, Ezra Wiater, Pasquapina Ciarmela, Wataru Wata, Karsten Schmidt, Joan Vaughan, Kathy Lewis, Amy Blount and Jessica Reed. I would also like to thank the following members for their intellectual contributions to my research: Marylin Perrin, Sean Smith, Chien Li, Alon Chen, Nick Justice, Bhawanjit Brar, Mark Huising, Talitha van der Muelen, Samantha Dettloff, Anna Pilbrow, Jacqueline Farber, Brooke Henry, Cindy Donaldson, Kathy Falkenhagen and Remy Manuel. In addition to

the scientific staff, there are several individuals whose efforts facilitate the proper functioning of the Vale Lab on a day-to-day basis. I would like to thank the following people for their administrative and technical assistance: Sandra Guerra, Debbie Johns and Dave Dalton.

I would also like to thank the members of my dissertation committee (Alexander Hoffmann, Daniel Donoghue, Peter Wolynes, and Shunichi Shimasaki) who have given me significant guidance as I've progressed through my graduate studies.

Recently, I have had the opportunity to establish a productive collaboration with Athanasia Panopoulos in the laboratory of Juan Carlos Izpisua Belmonte at the Salk Institute. I am grateful for their willingness to collaborate on projects addressing the role of Cripto and GRP78 in human embryonic stem cells. Their scientific expertise and intellectual contributions have added significantly to the impact of this work.

Throughout my graduate studies, I have had the unique opportunity to train with Peter Gray, a Staff Scientist in the Vale Lab. Peter has been an impeccable mentor during my graduate studies. His intellectual and scientific accomplishments are many and it has been a distinct privilege to work closely with Peter. In addition to the outstanding collaboration that we have developed during my graduate studies, Peter has is a great friend. I look forward to when and where our scientific paths cross next.

Chapter 1, in full, contains text and data published in the Journal of Biological Chemistry, 2008 Feb 22;283(8):4490-500 (with Shani G, Booker EC, Vale WW, Gray PC). The disseratation author was the primary investigator and author of this report.

Chapter 2, in full, contains text and data in preparation for publication (with Panopoulos AD, Shani G, Booker EC, Belmonte JC, Vale WW, Gray PC). The disseratation author is the primary investigator and author of this report.

I want to thank my family. My mom and step-dad, Linda and Ray, have been unwavering supporters of Julie and me, and we are so thankful for your strong belief in God. I am also thankful for my dad and brother, Jim and Noah. It has been a joy to learn to know you both better. My brothers and sister, Gary, Chad and Kim, have loved and encouraged Julie and me over the past eleven years – thank you. I would also like to thank Julie's sisters, their husbands and Julie's mom (Jan) and Dad (Alex). They have supported and encouraged us both in very meaningful ways during these first years of our marriage. We consider ourselves very blessed to have such a wonderful family. In addition to my immediate family, Julie and I have been blessed with two wonderful church communities and I'd like to thank our families at Clairemont Emmanuel and Glenkirk.

Finally, I want to give credit and honor to God, through whom I find strength to sustain my journey in these exhilarating, uncertain and uncharted territories of science.

VITA

1999 Bachelor of Science, Chemistry, California State Polytechnic, Pomona

1999-2002 Teacher at The Webb Schools, Claremont

2003 Master of Science, Biochemistry, California State Polytechnic, Pomona

2002-2004 Teaching Assistant, Chemistry/Biochemistry California State Polytechnic, Pomona

2004-2005 Teaching Assistant, Chemistry/Biochemistry, University of California, San Diego

2009 Doctor of Philosophy, Chemistry/Biochemistry, University of California, San Diego

PUBLICATIONS

Kelber, J. A., Panopolous, A. D., Shani, G., Booker, E.C., Belmonte, J.C., Vale, W.W., Gray, P.C. *Blockade of Cripto binding to cell surface GRP78 inhibits oncogenic Cripto signaling via MAPK/PI3K and Smad2/3 pathways* (2009) In preparation

Kelber, J.A., Shani, G., Booker, E.C., Vale, W.W., Gray, P.C. *Cripto is a noncompetitive activin antagonist that forms analogous signaling complexes with activin and nodal* (2008) J Biol Chem 283(8), 4490-4500

Shani, G., Fischer, W.H., Justice, N.J., Kelber, J.A., Vale, W.W., Gray, P.C. *GRP78 and Cripto form a complex at the cell surface and collaborate to inhibit transforming growth factor beta signaling and enhance cell growth* (2008) Mol Cell Biol 28(2), 666-677

Gray, P.C., Shani, G., Aung, K., Kelber, J.A., Vale, W.W. *Cripto binds transforming growth factor beta (TGF-beta) and inhibits TGF-beta signaling* (2006) Mol Cell Biol 24, 9268-78

Mobley, P.W., Nisthal, A., Julius, J., Kelber, J.A., Gonzales, A., Eskandari, S., Waring, A., Gordon, L. *The HIV-1 fusion peptide has amyloid properties* (2006) Proceedings of the 19th American Peptide Symposium 9, 686-687

FIELDS OF STUDY

Cell Biology/Biochemistry of Cancer

TGF-β, MAPK and PI3K signal transduction pathways as they relate to tumor growth and metastasis

Wylie Vale (The Salk Institute for Biological Studies)

ABSTRACT OF THE DISSERTATION

Mechanism, Function and Modulation of Oncogenic Cripto Signaling

by

Jonathan A. Kelber

Doctor of Philosophy in Chemistry

University of California, San Diego, 2009

Professor Wylie Vale, Chair

Professor Alexander Hoffmann, Co-Chair

Cripto is a multifunctional protein with key roles during embryonic development and tumorigenesis. Cripto's oncogenic functions have been linked to its regulation of TGF-β ligand signaling via the Smad2/3 pathway and its growth factor activity via the MAPK/PI3K pathways. Notably, Cripto is required for signaling by certain TGF-β superfamily members such as Nodal, but also antagonizes others such as activin and TGF-β. The opposing effects of Cripto on Nodal and activin signaling seem contradictory, however, since these closely related ligands utilize the same receptors. Chapter one addresses this apparent paradox by demonstrating that Cripto

forms analogous receptor complexes with Nodal and activin and functions as a non-competitive activin antagonist. The results show that activin-A and Nodal elicit similar maximal signaling responses in the presence of Cripto that are substantially lower than that of activin-A in the absence of Cripto. In addition, biochemical data reveal complexes containing activin-A, Cripto and both receptor types and show that the assembly of such complexes is competitively inhibited by Nodal. Furthermore, both Nodal and activin-A share the same binding residues on ActRII. Finally, data presented here demonstrate that the ALK4 ECD has distinct and separable binding sites for activin-A and Cripto. Importantly, ALK4 ECD mutants with disrupted activin-A binding can bind and block Cripto effects on both activin-A and Nodal signaling. We recently demonstrated that Cripto forms a cell surface complex with glucose-regulated protein-78 (GRP78). Chapter two provides evidence that shRNA knockdown or immunoneutralization of GRP78 inhibits the ability of Cripto to function as a Nodal co-receptor, an antagonist of activin and TGF-β signaling and an activator of MAPK/PI3K pathways. Disrupting the Cripto/GRP78 complex also prevents Cripto from increasing cellular proliferation, downregulating E-Cadherin, decreasing cell adhesion and promoting mitogenic activin-A and Nodal signaling. The results indicate that GRP78 is a critical mediator of Cripto signaling in human tumor, mammary epithelial and embryonic stem cells and suggest that the Cripto/GRP78 complex

plays key roles during normal developmental processes and tumorigenesis. Collectively, the work presented in this dissertation represents seminal advances in understanding the mechanism and function of Cripto-mediated signaling.

INTRODUCTION

Cripto, also known at teratocarcinoma-derived growth factor (TDGF), is the founding member of the epidermal growth factor-like (EGF-like) – Cripto FRL1 Cryptic (CFC) family of glycophosphatidylinositol (GPI) anchored proteins. Members of this family of proteins typically contain two functional domains. The N-terminal EGF-like domain mediates the ability for EGF-CFC proteins to bind transforming growth factor – beta (TGF-β) superfamily ligands such a activins, Nodal and TGF-β1. Furthermore, a synthetic peptide corresponding to this domain (p47) has been demonstrated to activate the mitogen-activated protein kinase (MAPK) and phosphoinositide 3-kinase (PI3K) pathways. Additionally, the C-terminal CFC domain of Cripto mediates its ability to bind to the type I activin receptor, activin-like kinase 4 (ALK4, ActRIB) and to cell surface populations of glucose-regulated protein 78 (GRP78, BiP). Cripto plays essential roles during development as exemplified by the embryonic lethal phenotype displayed by Cripto null mice. These mice die as early as embryonic day 7.5. Based upon this essential role of Cripto during development, it is not surprising that Cripto expression is also elevated in mouse and human embryonic stem cells. In this context, Cripto has been reported to be a key marker for stem cell pluripotency and can also mediate the directed differentiation toward mesendoderm-derived germ layers. While Cripto is expressed at high levels in multiple contexts during

development, it is relatively undetectable in healthy adult tissues. Recent evidence has demonstrated that Cripto is expressed in the adult macaque brain, but the function of Cripto in this context is unknown. Importantly, evidence points to key role for Cripto in promoting the tumor phenotype in adult tissues. Not only is Cripto expression elevated in multiple tumor types in relation to its expression levels in the same healthy tissues, but Cripto can also transform cells derived from healthy tissues as well as those same tissues *in vivo*. As an example, Cripto promotes hyperplasia in healthy breast tissue when its overexpression is driven by the mouse mammary tumor virus (MMTV) promoter. As a result of these previous studies, Cripto has been designated as a developmental oncoprotein.

Tumor growth and spread is a multi-step process that ultimately results in the metastasis of primary tumor cells to remote locations in the body. The metastatic process presents significant hurdles in fighting cancer as this is an indication that the cancer cells have detached from the site of the primary tumor and entered the circulatory or lymph system. Consequently, it is a major interest of cancer biologists to understand the cellular and molecular events that drive the growth and metastasis of primary tumor cells. Furthermore, developing diagnostics aimed at early detection of tumors and therapies that target the growth and metastatic stages are central in the fight against cancer. Cripto has been implicated in promoting the characteristic

stages of cancer growth and spread. Cripto has been demonstrated to promote hyperproliferation and neovascularization of primary tumor cells. Furthermore, Cripto promotes cellular migration and down-regulation of cell-cell adhesion molecules such as E-Cadherin. These processes are hallmarks of epithelial-to-mesenchymal (EMT) transition – a necessary precursor for metastasis in epithelial-derived cancers. Notably, monoclonal antibodies raised against the EGF-like or CFC domains of Cripto have been reported to inhibit the tumorigenic properties of Cripto-expressing cells when they are orthotopically implanted into immune-deficient mice.

Cripto has been reported to regulate the signaling activity of key pathways that have been demonstrated to promote tumor growth and spread. Cripto regulates ligand-dependent receptor assembly and signaling activity by TGF-β ligands. These ligands are ubiquitous regulators of cellular function. They are structurally-related polypeptides that play key roles in tissue development and homeostasis during development and in the adult. Not surprisingly, dysregulation of signaling by these ligands can lead to a number of pathophysiological conditions, including cancer. Initially, Cripto was demonstrated to be a required co-receptor for Nodal (and Nodal-like ligands such as GDF-1 and Vg-1) to assemble with the activin type II (ActRII/IIB) and type I (ALK4) receptors to induce Smad 2 or Smad 3 phosphorylation. Importantly, Cripto can bind to the ALK4 receptor

independent of ligand binding, but Nodal can not bind to these receptors without Cripto. In addition to the necessary developmental processes that require Cripto-dependent Nodal signaling, this pathway has been recently implicated in promoting late stage melanoma metastasis. Following on the heels of these studies, our group and others have demonstrated that Cripto antagonizes activin and TGF-β1 signaling activity. Importantly, activin and Nodal activate Smad 2 or Smad 3 through the assembly of the same signaling receptors, ActRII/IIB and ALK4. Therefore, it is instructive to consider the mechanism by which Cripto antagonizes activin signaling, but facilitates Nodal signaling. Chapter one of this dissertation attempts to address the mechanism by which Cripto modulates activin and Nodal signaling. Base upon the data, we have concluded that Cripto is a noncompetitive activin antagonist that forms analogous signaling complexes with activin and Nodal. Cripto's ability to modulate signaling levels by activins, Nodal and TGF-β may contribute in part to its ability to promote uncontrolled growth of tumor cells. Interestingly, dysregulated Smad2/3 signaling has been correlated with hyperproliferation and metastasis of tumor cells.

In addition to impacting the Smad2/3 signaling pathway, Cripto also promotes the tumor phenotype by activating the MAPK and PI3K pathways. Nevertheless, how extracellular populations of Cripto couple to the activation of these intracellular pathways has remained unclear.

Interestingly, Cripto has been reported to activate tyrosine phosphorylation of the type IV EGF receptor (ErbB-4). However, it was not demonstrated to bind this receptor. While Cripto was also shown to coimmunoprecipitate with the heparin-binding proteoglycan Glypican-1 and intracellular populations of phosphorylated Src, the coupling of extracellular Cripto to intracellular Src is still not explained by these protein-protein interactions. Finally, the hypothesis that Cripto could activate the MAPK and PI3K pathways via its ability to bind to the type I activin receptor (ALK4) was tested and it was reported that Cripto could activate these pathways independent of the ALK4 intracellular kinase domain. Consequently, how Cripto activates the MAPK and PI3K pathway has remained elusive. Early in 2008, our group identified the endoplasmic reticulum chaperone, glucose-regulated protein 78 (GRP78), as a critical cell surface Cripto binding protein. Furthermore, we showed that GRP78 enhanced Cripto's ability to antagonize TGF-β signaling and promote cellular growth. Chapter two of this dissertation attempts to address whether or not GRP78 is necessary for other functions of Cripto. Specifically, we show that cell surface GRP78 is necessary for Cripto-mediated signaling via the MAPK/PI3K and Smad2/3 pathways.

CHAPTER 1

CRIPTO IS A NONCOMPETITIVE ACTIVIN ANTAGONIST THAT FORMS ANALOGOUS SIGNALING COMPLEXES WITH ACTIVIN AND NODAL

INTRODUCTION

The transforming growth factor β (TGF-β) superfamily contains approximately 40 structurally related ligands that control a wide range of diverse cellular processes including proliferation, homeostasis, differentiation and migration (Massague and Gomis, 2006; Pardali and Moustakas, 2007). TGF-β ligands exert their biological effects by binding and assembling two types of transmembrane receptors (type I and type II) with intrinsic serine/threonine kinase activities (Schmierer and Hill, 2007; Shi and Massague, 2003). There are five type II receptors and seven type I receptors and therefore these receptors display varying degrees of promiscuity with regard to the ligands they bind (Shi and Massague, 2003). Activin type II (ActRII and ActRIIB) and type I (ALK4) receptors are especially promiscuous and form signaling complexes with activins but also several other superfamily members including GDF1, GDF3, GDF8 (myostatin) and Nodal (Harrison et al., 2005). In cases where multiple TGF-β ligands share the same receptors, signaling specificity can be achieved via ligand

specific differences including variable expression patterns, processing of mature ligands from pro-peptides, stabilities, receptor affinities, susceptibility to extracellular ligand traps, and modulation by co-receptor proteins (Piek et al., 1999; Schmierer and Hill, 2007; Shi and Massague, 2003).

As an example, activin and Nodal utilize the same signaling receptors but their mechanisms of ligand-mediated receptor assembly and use of co-receptor proteins differ significantly. On the one hand, activins initiate signaling by first binding ActRII/IIB with high affinity (Attisano et al., 1992; Mathews and Vale, 1991; Mathews et al., 1992) and then recruiting ALK4 resulting in the formation of active signaling complexes (Carcamo et al., 1994; Tendijke et al., 1994). By contrast, Nodal lacks intrinsic affinity for ActRII/IIB and ALK4 and requires Cripto (Cripto-1, TDGF1) or a related co-receptor to facilitate its binding to these receptors (Schier, 2003; Shen, 2007; Yeo and Whitman, 2001). Cripto is a small, GPI-anchored protein that possesses two modular cysteine rich domains, an EGF-like domain that binds Nodal and a CFC domain that binds ALK4 (Schier, 2003; Shen and Schier, 2000; Strizzi et al., 2005). Structure/function studies have shown that Nodal assembles type II and type I receptors only in the presence of Cripto. In fact, disruption of Nodal binding to the EGF-like domain or ALK4 binding to the CFC domain completely abolishes Cripto-dependent Nodal signaling (Minchiotti et al., 2001; Yan et al., 2002; Yeo and

Whitman, 2001). Following receptor assembly, propagation of activin and Nodal signals is thought to be essentially the same, i.e. ALK4 is phosphorylated and activated by the constitutively active ActRII/ActRIIB receptor kinase and in turn phosphorylates cytoplasmic Smad2 and Smad3 proteins. Once phosphorylated, Smad2 and Smad3 assemble into complexes together with Smad4 and then migrate into the nucleus where they interact with transcription factors, co-activators and co-repressors to regulate transcription of target genes (Shi and Massague, 2003).

In contrast to its requirement for Nodal signaling, Cripto has been shown to antagonize activin signaling apparently by preventing activin from assembling its receptors (Shen, 2003). For example, we have demonstrated that Cripto forms complexes with activin-A and ActRII/IIB and reduces activin-A crosslinking to ALK4 (Gray et al., 2003). This observation led us to propose a model in which Cripto inhibits activin-A signaling by competing with ALK4 for access to activin-A/ActRII/IIB complexes. Cripto was also shown to bind activin-B, and in this case it was proposed that Cripto inhibits activin-B signaling by forming non-productive complexes with activin-B and/or ALK4 (Adkins et al., 2003). While these studies reported distinct inhibitory complexes, they each presented models in which Cripto competitively inhibits activin signaling by blocking receptor assembly. Notably, these models appear to be incompatible with the well-

documented role of Cripto as a Nodal co-receptor that facilitates receptor assembly. Specifically, it remains unclear how Cripto can form functional signaling complexes with Nodal while inhibiting activin-dependent receptor assembly.

In the present study, we provide evidence supporting a new model that explains the seemingly contradictory effects of Cripto on activin and Nodal signaling. We demonstrate that Cripto is a non-competitive activin antagonist and that activin and Nodal assemble Cripto-containing receptor complexes that are structurally and functionally similar. We also identify ALK4 mutants that bind Cripto and block its effects on activin-A and Nodal signaling. Together, our data suggest that Cripto functions as a molecular switch that causes cellular responses to activin and Nodal to converge via the formation of analogous signaling complexes.

MATERIALS AND METHODS

Materials. NuPAGE gels and molecular weight markers were obtained from Invitrogen. Recombinant human activin-A was generated using a stable activin-A-expressing cell line generously provided by Dr. J. Mather (Genentech, Inc., South San Francisco, CA) and was purified by Wolfgang Fischer (Peptide Biology Laboratory, Salk Institute, La Jolla, CA). Recombinant mouse Nodal were purchased from R&D Systems. ^{125}I-Activin-A was prepared using the chloramine T method as described previously (Vaughan and Vale, 1993). Anti-myc (9E10)

monoclonal antibody and protein G agarose were purchased from Calbiochem. Polyclonal antibodies directed against ALK4 (Tsuchida et al., 1995) have been described. A polyclonal anti-Cripto antibody (6900) was produced in rabbits immunized with a peptide from the EGF-like domain of Cripto (C_{82}PPSFYGRNCEHDVRKE$_{98}$). Anti-Flag (M2) antibody and Flag (M2) agarose were from Sigma. Anti-Phospho-Smad2, anti-Smad2/3, and anti-pan Actin antibodies were purchased from Cell Signaling Technologies (Danvers, MA). Horseradish peroxidase-linked anti-rabbit IgG, anti-mouse IgG, 3,3',5,5'-tetramethylbenzidine (TMB) substrate, chemiluminescent substrate (SupersignalTM), and the BCA protein assay kit were obtained from Pierce. All DNA constructs used in this study were in the pcDNA3.0 expression vector (Invitrogen).

Expression Constructs. The mouse Cripto construct has been described (Yeo and Whitman, 2001) and was a generous gift from Malcolm Whitman (Department of Cell Biology, Harvard Medical School, Boston, MA). The ΔCFC Cripto deletion mutant was generated using a previously described PCR strategy (Harms and Chang, 2003) in which the CFC domain was replaced with an in-frame BamHI site (GGATCC) encoding the amino acids Gly-Ser. The kinase-deleted ALK4 constructs (ALK4-trunc) encode the first 206 amino acids of ALK4 and were generated using standard PCR techniques as previously described (Harrison et al., 2003). Similar standard PCR

strategies were used to make kinase-deleted ActRII constructs (ActRII-trunc) and to introduce epitope tags (Gray et al., 2000; Harrison et al., 2003). All constructs were confirmed by DNA sequencing.

Transfection and Detection of Cell Surface Protein Expression in HEK 293T Cells. HEK 293T cells were grown in 5% CO_2 to 40-60% confluence in complete Dulbecco's modified Eagle's medium (with 10% bovine calf serum, penicillin, streptomycin, and L-glutamine) on poly-D-lysine-coated wells or plates. Cells were transfected with indicated DNA constructs using Perfectin (Gene Therapy Systems). For Western blotting, cells were solubilized in RIPA buffer (50 mM Tris-HCl, pH 7.4, 150 mM NaCl, 1% NP-40, 0.5% deoxycholate and 0.1% sodium dodecyl sulfate) containing standard protease inhibitors. SDS-PAGE and electrotransfer to nitrocellulose were carried out using NuPAGE gels and a NOVEX X-cell II apparatus as described previously (Gray et al., 2000). To detect proteins expressed at the cell surface, intact cells were washed with Hepes Dissociation Buffer (HDB), blocked with 3% BSA/HDB, incubated with anti-Flag antibody, washed with HDB, and incubated with peroxidase-conjugated anti-mouse IgG. Specific antibody staining was measured using the TMB peroxidase substrate as described previously (Gray et al., 2000).

Luciferase Assays. Luciferase assays were carried out using the A3-luciferase reporter essentially as previously described (Gray et

al., 2003). The A3-luciferase construct contains three copies of the ARE (activin response element) from the *Xenopus laevis Mix.2* promoter linked to a basic TATA box and a luciferase reporter gene. HEK 293T cells were plated on poly-D-lysine-coated 24-well plates at $1x10^5$ cells per well and transfected (Perfectin) in triplicate approximately 24 h later with 500 ng of DNA per well using 10-400 ng of DNA contructs (indicated combinations of pcDNA 3.0 vector, Cripto, WT or mutant ActRII-trunc and WT or mutant ALK4-trunc) and 50 ng FAST2 (FoxH1)/25 ng A3-luciferase/25 ng CMV-β-galactosidase. Cells were treated approximately 24 h following the transfection and then harvested approximately 16 h following treatment. Cells were incubated in solubilization buffer (1% Triton X-100, 25 mM glycylglycine [pH 7.8], 15 mM $MgSO_4$, 4 mM EGTA, and 1 mM dithiothreitol (DTT)) for 30 min on ice and luciferase reporter activity was measured and normalized relative to CMV-β-Gal activities.

Smad2 Phosphorylation. HEK 293T cells were plated on six-well plates at a density of $2x10^5$ cells per well. 24 h after plating, cells were transfected with 2 g of DNA (1 μg vector and 1 μg Cripto) using Perfectin. 24 h after transfection, cells were serum-starved overnight prior to treatment. Cells were left untreated or treated for 30 minutes indicated doses of activin-A or Nodal. Cells were harvested by adding 150 μl ice-cold RIPA buffer (50 mM Tris-HCl, pH 7.4, 150 mM NaCl, 1% NP-40, 0.5% deoxycholate, 0.1% sodium dodecyl sulfate)

supplemented with 50mM β-glycerol phosphate, 20 mM NaF, and standard protease inhibitors. Fifty μL of 4X SDS-PAGE loading buffer was than added to each sample and the proteins were separated by SDS-PAGE and blotted to nitrocellulose. Blots were treated with anti-phospho-Smad2 or anti-Smad2/3 antibodies followed by anti-rabbit IgG antibody conjugated to horseradish peroxidase and bands were detected using enhanced chemiluminescence.

Covalent Crosslinking. HEK 293T cells were plated on six-well plates coated with poly-D-lysine at a density of $4x10^5$ cells per well. Approximately 24 h later, cells were transfected with 2 μg of DNA per well (1 μg of ActRII-myc, 0.5 μg of ALK4-untagged and 0.5μg of WT-Flag) using Perfectin and then incubated an additional 48 h before harvesting. Covalent crosslinking was performed by first washing cells in HDB (12.5 mM Hepes, pH 7.4, 140 mM NaCl, 5 mM KCl) and then incubating cells with ^{125}I-activin-A in binding buffer (HDB containing 0.1% BSA, 5 mM $MgSO_4$, 1.5 mM $CaCl_2$) at room temperature for 4 h. Cells were washed with HDB and incubated in 0.5 mM disuccinimidyl suberate (DSS) in HDB for 30 min on ice. Crosslinking reactions were quenched with TBS (50 mM Tris-HCl/pH 7.5, 150 mM NaCl) and then cells were solubilized in lysis buffer (TBS containing 1% Nonidet P-40, 0.5% deoxycholate, 2 mMEDTA) with lysates subjected to immunoprecipitation by using anti-myc, anti-Flag, or anti-ALK4 antibodies. Immune complexes were then analyzed by SDS-PAGE and

autoradiography. For Nodal competition, cells were pretreated with 100 nM Nodal for 30 minutes prior to incubating cells with ^{125}I-activin-A tracer.

Alternatively, P19 emrbyonal carcinoma cells (ECCs) were plated on 10 cm plates coated with poly-D-lysine at 2x10^5 cells per well. Approximately 48 h later, covalent crosslinking was performed by first washing cells in HDB, treating with 10 nM cold activin-A or leaving cells untreated, and then incubating cells with ^{125}I-activin-A in binding buffer at room temperature for 2 h. Cells were washed with HDB and incubated in 0.5 mM DSS in HDB for 30 min on ice. Crosslinking reactions were quenched with TBS and cells were solubilized in lysis buffer. Lysates were subjected to immunoprecipitation using anti-Cripto or non-specific rabbit IgG antibodies. Immune complexes were then analyzed by SDS-PAGE and autoradiography.

Co-Immunoprecipitation and Western Blot Analysis. 1x10^6 HEK 293T cells were plated in 10 cm plates. Approximately 24 h later, cells were transfected with 12 μg DNA per plate (6 μg vector or untagged WT or ΔCFC Cripto and 6 μg vector or Flag-tagged WT or mutant ALK4-trunc) using polyethylimine (PEI) and cells were incubated another 48 h before harvesting. Cells were lysed and scraped on ice in 0.8 mL of cold RIPA buffer (50 mM Tris-HCl, pH 7.4, 150 mM NaCl, 1% NP-40, 0.5% deoxycholate, and 0.1% sodium dodecyl sulfate) containing standard protease inhibitors. Cellular

lysates were precleared by centrifugation and 75 μL of the total lysates were heated and frozen in 4X SDS-PAGE loading buffer (with DTT), while the remainder of the lysates were incubated overnight at 4^{o}C with Flag (M2) agarose. Precipitated complexes were washed three times with cold RIPA buffer for 1 h each, eluted from beads and then subjected to SDS-PAGE and electrotransfer to nitrocellulose, followed by Western blotting using the Cripto antibody.

RESULTS

Cripto reduces maximal activin-A-dependent luciferase induction to a level that converges with that of Nodal. In order to compare the roles of Cripto as a co-receptor for Nodal and an inhibitor of activin-A signaling, 293T cells were transfected with the Smad2-responsive luciferase reporter A3-Lux and FAST2 (FoxH1) in the presence of vector or Cripto and then treated with a range of doses of each ligand. Consistent with previous reports that Nodal requires Cripto as an obligatory co-receptor (Shen, 2007), we did not observe Nodal signaling in the absence of Cripto even at the highest dose of 180 nM Nodal (Figure 1A). By contrast, in the presence of Cripto, Nodal caused a dose-dependent induction of luciferase with an EC_{50} of ~14 nM and a maximal induction of ~20-fold basal (Figure 1A).

In parallel experiments, we measured the dose response relationship for activin-A in the absence or presence of Cripto. In the

absence of Cripto, maximal doses of activin-A elicited a robust ~40-fold induction of luciferase that was significantly larger than that observed in response to maximal doses of Nodal in the presence of Cripto (Figure 1A, B). Activin-A had an EC_{50} of ~60 pM and was therefore nearly 250 times more potent than Nodal (EC_{50} ~14 nM). Consistent with our previous findings (Gray et al., 2003), activin-A signaling was inhibited by the presence of Cripto and this inhibition was observed at each dose of activin-A tested (Figure 1B). However, the potency of activin-A in the presence of Cripto (EC_{50} of ~41 pM) was essentially the same as in the absence of Cripto (EC_{50} of ~60 pM) suggesting that activin-A affinity for the type II receptor (ActRII/IIB) was unaffected by Cripto. Notably, despite their disparate potencies, activin-A and Nodal displayed a similar maximal level of luciferase induction (~20 fold basal) in the presence of Cripto (Figure 1A, B). Thus, Cripto reduced the maximal signaling capacity of activin-A to a level similar to that of Nodal.

Next, we asked how the level of Cripto expression in these cells affects Nodal and activin-A signaling. 293T cells were transfected with a range of doses of the Cripto expression vector, treated with 30 nM Nodal or 250 pM activin-A and then resulting luciferase induction was measured. As shown in Figure 1C, Nodal signaling increased as the level of Cripto DNA was increased and this effect was mirrored by a corresponding decrease in the activin-A

response. Strikingly, as Cripto DNA doses were increased, Nodal and activin-A responses converged at ~20 fold basal (Figure 1C). The Nodal and activin-A responses were indistinguishable following transfection of 300 ng or 500 ng of Cripto DNA (Figure 1C), despite the fact that the level of cell surface Cripto expression was substantially higher following transfection with 500 ng Cripto DNA than it was following transfection of 300 ng (Figure 1D). Therefore, since maximal inhibition of activin-A signaling by Cripto was partial and achieved at submaximal Cripto levels, we conclude that Cripto is a non-competitive activin-A antagonist.

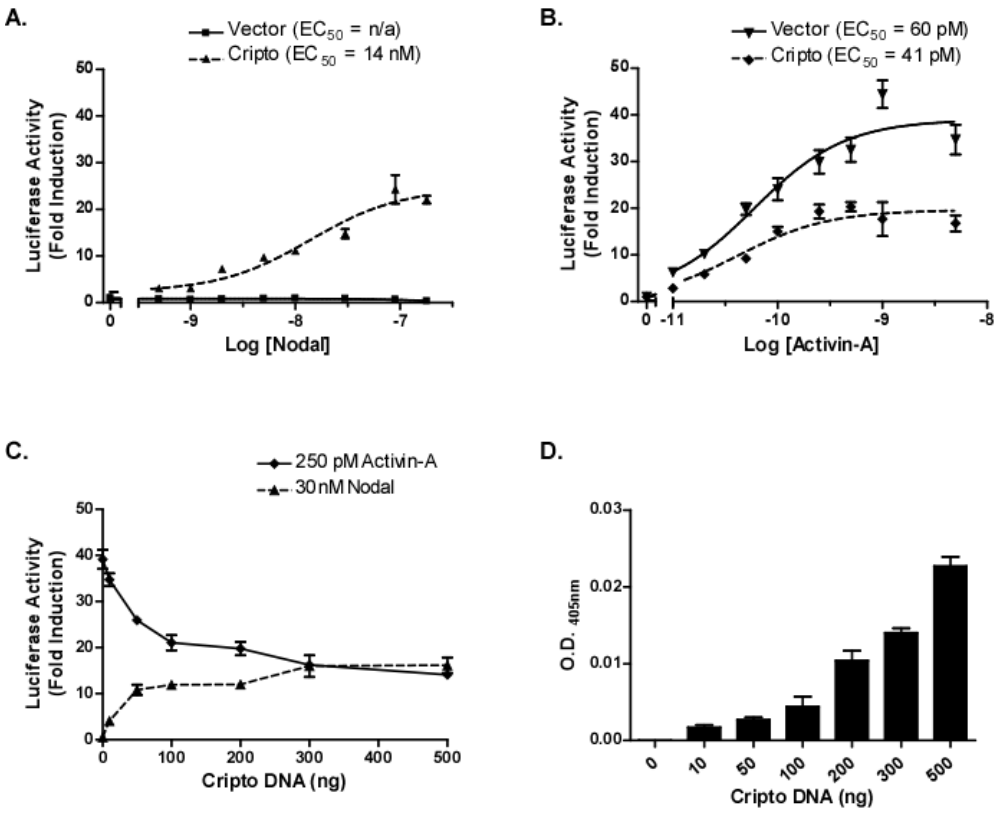

Figure 1: Cripto reduces activin-A efficacy to a level similar to that of Nodal. 293T cells were transfected with A3-lux, FAST2 and CMV-β-galactosidase. Resulting luciferase activities were normalized relative to β-galactosidase activities and are presented as fold induction. (A and B) Cells were further transfected with 200 ng of empty vector or Cripto plasmid as described under Experimental Procedures and were left untreated or treated with the specified doses of either Nodal or activin-A. (C) Cells were further transfected with indicated doses of Cripto plasmid as described under Experimental Procedures and either left untreated or treated with 250 pM activin-A or 30 nM Nodal. In (D) cells were again transfected with the indicated doses of Cripto DNA and cell surface expression was measured using an intact cell ELISA assay as described under Experimental Procedures.

Cripto reduces activin-A-induced Smad2 phosphorylation to a level similar to that of Nodal. In order to further compare the effects of Cripto on activin-A and Nodal signaling, we measured the relative ability of these ligands to activate Smad2 phosphorylation in the absence or presence of Cripto. In agreement with the luciferase data presented above, we have shown that transfection of Cripto is

necessary for Nodal induced Smad2 phosphorylation (Figure 2). By contrast, activin-A induced robust Smad2 phosphorylation in these cells in the absence of Cripto. Importantly, and consistent with the luciferase assays, transfection of Cripto into these cells reduced the extent of activin-A-induced Smad2 phosphorylation to a level resembling that of Nodal (Figure 2).

In summary, three novel conclusions can be drawn from these data measuring the effects of Cripto on Nodal and activin-A signaling: 1) Activin-A has a higher intrinsic efficacy than Nodal; 2) Cripto does not change the potency (EC_{50}) of activin-A but rather acts in a non-competitive manner to reduce activin-A efficacy; and 3) the efficacies of activin-A and Nodal converge as Cripto expression increases.

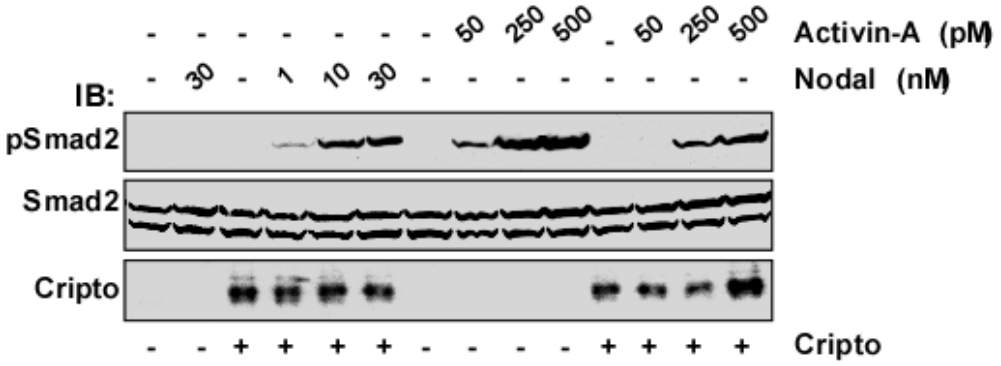

Figure 2: Cripto reduces activin-A-induced Smad2 phosphorylation to a level similar to that of Nodal. 293T cells were transfected with empty vector or Cripto and treated with the indicated doses of Nodal or activin-A. Resulting cell lysates were subjected to Western blotting using anti phospho-Smad2, anti-Smad2 or Cripto antibodies as described under Experimental Procedures.

Activin-A assembles complexes containing ActRII, ALK4 and Cripto. The similar magnitudes of activin-A and Nodal signaling responses in the presence of Cripto suggested that these ligands

form structurally similar complexes containing Cripto and both receptor types. To test this, we transfected 293T cells with ActRII-myc, ALK4 and/or Cripto-Flag constructs as indicated (Figure 3), labeled them with ^{125}I-activin-A and then subjected them to covalent crosslinking. Resulting cell lysates were then subjected to immunoprecipitation using antibodies targeting ActRII-myc (Figure 3A), ALK4 (Figure 3B), or Cripto-Flag (Figure 3C). As expected, anti-myc immunoprecipitation of ActRII led to the isolation of ^{125}I-activin-A-labeled ActRII (lane 2), ActRII and ALK4 (lane 3), ActRII and Cripto (lane 4) and ActRII, ALK4 and Cripto (lane 5) (Figure 3A). While Cripto reduced crosslinking of activin-A to ALK4, it is notable that Cripto does not completely abolish this interaction raising the possibility that Cripto may exist in a complex with activin-A and both receptor types (Figure 3A, compare lanes 3 and 5). However, since ActRII was the target in the immunoprecipitation, we could not rule out the possibility that the labeled bands corresponding to ALK4 and Cripto (Figure 3A, lane 5) were derived from distinct complexes consisting of activin-A/ActRII/Cripto or activin-A/ActRII/ALK4. This issue was resolved by immunoprecipitation with an anti-ALK4 antibody that resulted in the clear detection of labeled bands corresponding to ActRII, ALK4 and Cripto (Figure 3B, lane 3). Since ALK4 and Cripto do not bind activin-A in the absence of ActRII (Gray et al., 2003), this result demonstrates that activin-A, ActRII, ALK4 and

Cripto are each indeed present in the same complexes. This finding was further confirmed by our visualization of bands corresponding to ^{125}I-activin-A labeled ActRII, ALK4, and Cripto following anti-Flag immunoprecipitation (Figure 3C, lane 3).

Having shown that activin-A can form complexes with ActRII, ALK4 and Cripto when they are overexpressed in 293T cells, we attempted to demonstrate the formation of these complexes in cells expressing these proteins at endogenous levels. Mouse embryonal carcinoma P19 cells express relatively high levels of endogenous Cripto and we therefore subjected these cells to ^{125}I-activin-A labeling, covalent crosslinking, and immunoprecipitation using an antibody that targets Cripto. To control for non-specific immunoprecipitation effects of rabbit anti-sera, we assessed the ability of rabbit IgG to immunoprecipitate similar complexes. As shown in Figure 3D, ^{125}I-activin-A-labeled bands corresponding to ActRII, ALK4, and Cripto were visualized following immunoprecipitation with an anti-Cripto antibody but not with non-specific IgG (Figure 3D). Furthermore, the appearance of these labeled bands was almost completely abolished when cells were pre-incubated with 10 nM unlabeled activin-A. Significantly, this is the first evidence that demonstrates that activin-A can form receptor complexes that contain endogenous ActRII, ALK4, and Cripto.

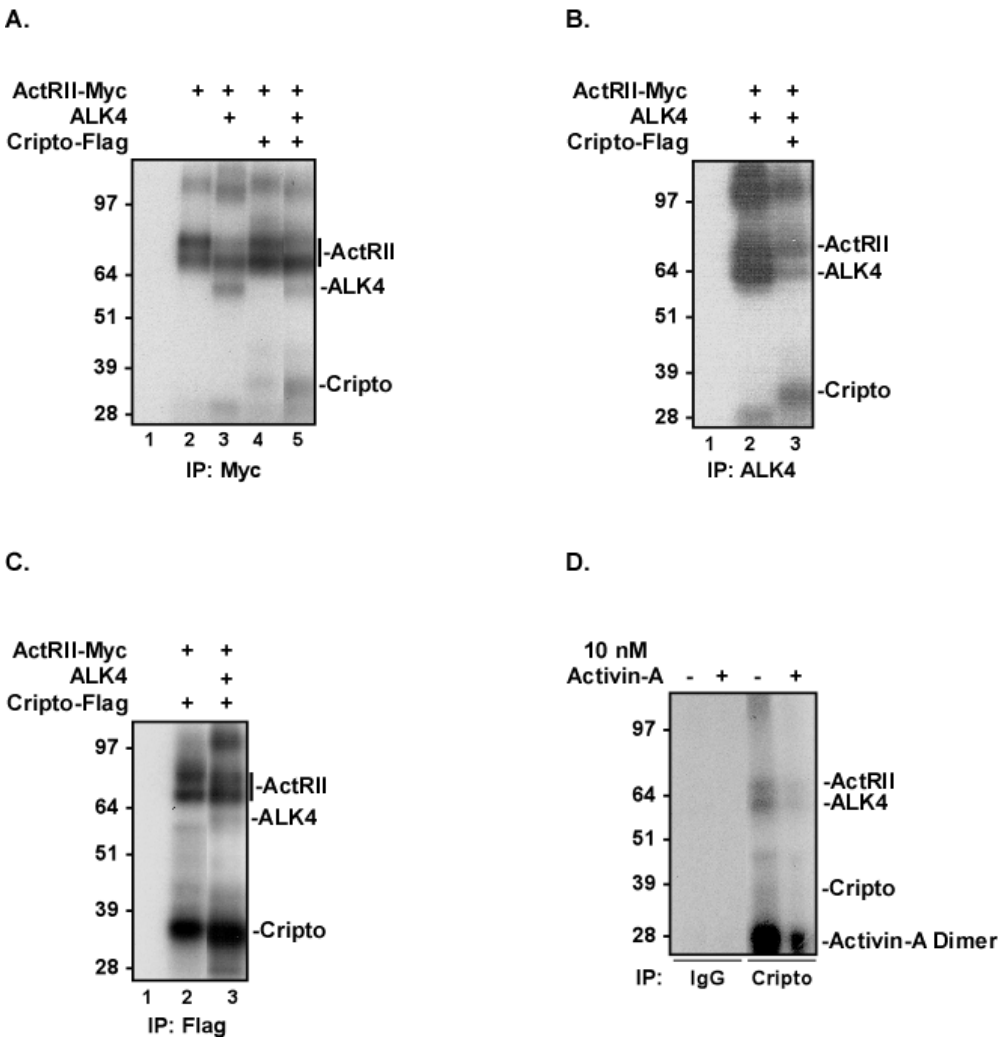

Figure 3: Activin-A forms a complex with ActRII, ALK4 and Cripto. 293T cells transfected with the indicated receptor or Cripto constructs (A-C) or native P19 cells (D) were subjected to ^{125}I-Activin-A crosslinking as described under Experimental Procedures. Crosslinked complexes were subjected to immunoprecipitation using antibodies targeting ActRII-Myc (A), ALK4 (B), Cripto-Flag (C) or native Cripto (D) and immune complexes were resolved via SDS-PAGE and visualized by autoradiography.

Nodal competes with activin-A for the formation of Cripto/ActRII/ALK4 complexes. Our results indicate that, like Nodal, activin-A can form complexes that contain both receptor types and Cripto. Given the apparent similarity of Cripto-containing activin and Nodal complexes, we reasoned that Nodal and activin-A might

compete with each other to assemble receptor complexes containing Cripto. To test this possibility, 293T cells were transfected with the indicated constructs (Figure 4A) and then subjected to ^{125}I-activin-A labeling in the absence or presence of 100 nM Nodal. As shown in Figure 4A, pretreatment of cells with 100 nM Nodal substantially decreased the intensity of ^{125}I-activin-A labeled receptor and Cripto bands, as visualized following Cripto immunoprecipitation, indicating that Nodal competitively disrupted the formation of both activin-A/ActRII/Cripto (Figure 4A, lanes 3 and 4) and activin-A/ActRII/ALK4/Cripto complexes (Figure 4A, lanes 5 and 6). Interestingly, Nodal competed with ^{125}I-activin-A crosslinking to Cripto in the absence of ALK4 further supporting previously published work demonstrating that Nodal can bind Cripto directly (Yeo and Whitman, 2001).

We predicted that activin-A and Nodal would not have additive signaling effects in the presence of Cripto since they apparently compete to form Cripto-containing receptor complexes that elicit similar signaling responses. To test this directly, we asked whether Nodal could increase the activin-A response in the absence or presence of Cripto. 293T cells were transfected with 400 ng of vector or Cripto and then treated with 100 pM activin-A, 30 nM Nodal or 100 pM activin-A plus 30 nM Nodal. As shown in Figure 4B, in the absence of Cripto activin-A elicits a ~27-fold induction of luciferase and, as predicted,

Nodal has no signaling effect either alone or together with activin-A. In cells transfected with 400 ng of the Cripto construct, the activin-A response was inhibited to ~18-fold while Nodal caused an ~13-fold induction. Importantly, when these cells were treated with activin-A and Nodal together, the signaling response was essentially the same as that observed following treatment with activin-A alone, i.e. Nodal does not increase the activin-A signaling response in the presence of Cripto. These data are consistent with our crosslinking data and suggest that Nodal and activin-A compete for access to the Cripto-bound fraction of ALK4 to form similar, low-efficacy signaling complexes.

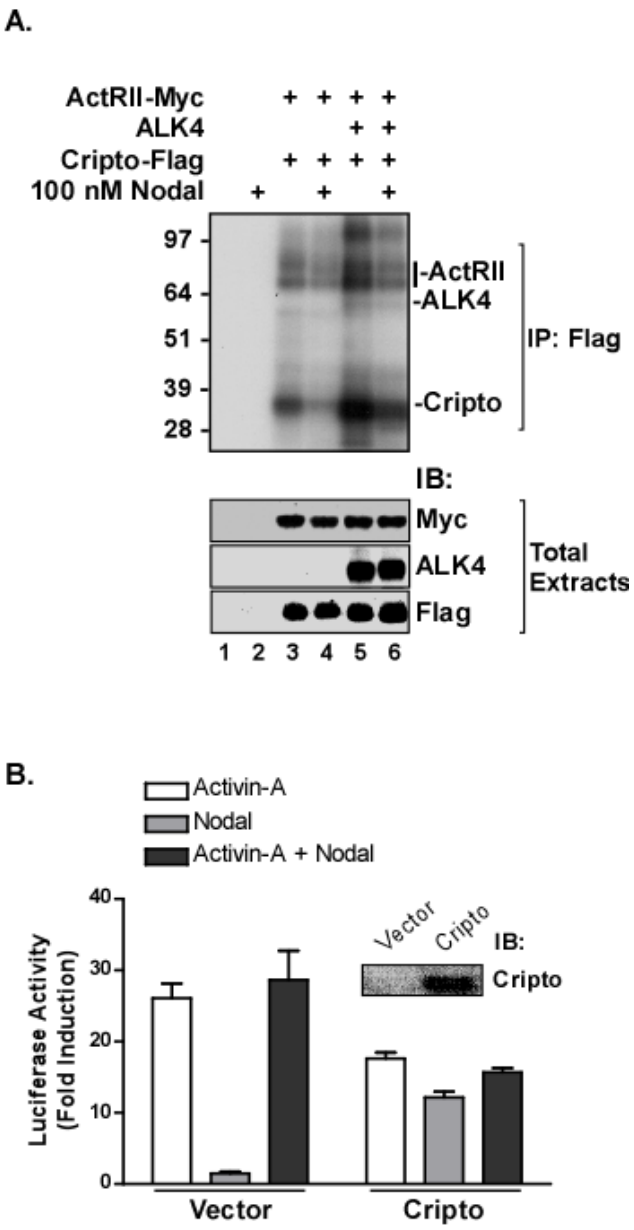

Figure 4: Nodal and activin-A compete to form complexes with ActRII, ALK4 and Cripto. (A) 293T cells were transfected with the indicated constructs, treated as indicated with 100 nM unlabeled Nodal and then subjected to ^{125}I-Activin-A crosslinking as described under Experimental Procedures. Crosslinked complexes were subjected to immunoprecipitation using antibodies targeting Cripto-Flag and then immune complexes were resolved via SDS-PAGE and visualized by autoradiography as described under Experimental Procedures. Corresponding protein levels from total cell extracts were determined by Western blot. (B) 293T cells were transfected with A3-lux, FAST2 and CMV-β-galactosidase together with 200 ng of empty vector or Cripto DNA as described under Experimental Procedures. Cells were treated with 100 pM activin-A, 30 nM Nodal or 100 pM activin-A plus 30 nM Nodal and resulting normalized luciferase activities are presented as fold induction.

Nodal and activin-A bind the same site on ActRII. Next, we probed the structural similarity of Nodal and activin-A signaling complexes in more detail by testing whether these ligands bind the same ActRII ECD residues. Activin-A binds a hydrophobic surface on the ActRII ECD consisting primarily of Phe^{42}, Trp^{60} and Phe^{83} and mutation of any one of these three residues to alanine abolishes binding (Gray et al., 2000). While the binding site for Nodal on ActRII has not yet been identified, it might be predicted to differ from that of activin-A since the ActRII-binding residues on activin-A are not conserved on Nodal and since Nodal binding to ActRII requires Cripto.

To determine whether Nodal binds the same surface on the ActRII ECD as activin-A, we used transmembrane, kinase-deleted ActRII (ActRII-trunc) constructs that bind cognate ligands, form non-productive ligand-receptor complexes and block signaling in a dominant negative manner (Chen et al., 1993; Hemmati-Brivanlou and Melton, 1992). We compared the abilities of wild type (WT) ActRII-trunc and the ActRII-trunc mutants F42A, W60A and F83A to block activin-A and Nodal signaling. As a control, we also tested the function of K56A ActRII-trunc since the K56A mutation did not affect activin-A binding to ActRII (Gray et al., 2000). 293T cells were transfected with empty vector, Cripto and various ActRII-trunc constructs as indicated, treated with 100 pM activin-A or 30 nM Nodal

and then resulting luciferase induction was measured. Cripto inhibited activin-A signaling and facilitated Nodal signaling as predicted such that both ligands signaled at a similar level in its presence (Figure 5). By contrast, the signaling response of both ligands was nearly abolished when WT ActRII-trunc and Cripto were co-transfected. Importantly, this result indicates that ActRII-trunc acts in a dominant negative manner to block signaling by both activin-A and Nodal in the presence of Cripto. As expected, the K56A ActRII-trunc mutant resembled WT ActRII-trunc in its ability to block activin-A signaling and it also blocked Nodal signaling. By contrast, the F42A, W60A and F83A ActRII-trunc constructs were only weakly able to inhibit signaling by both activin-A and Nodal indicating that in addition to disrupting activin-A binding, each of these ActRII ECD substitutions also prevents Nodal binding (Figure 5). Therefore, while activin and Nodal have distinct modes of accessing ActRII, these data indicate that both ligands interact with the same hydrophobic surface on ActRII constituted by Phe^{42}, Trp^{60} and Phe^{83}. This finding supports our model in which both activin-A and Nodal can form ActRII/ALK4/Cripto signaling complexes with similar structures.

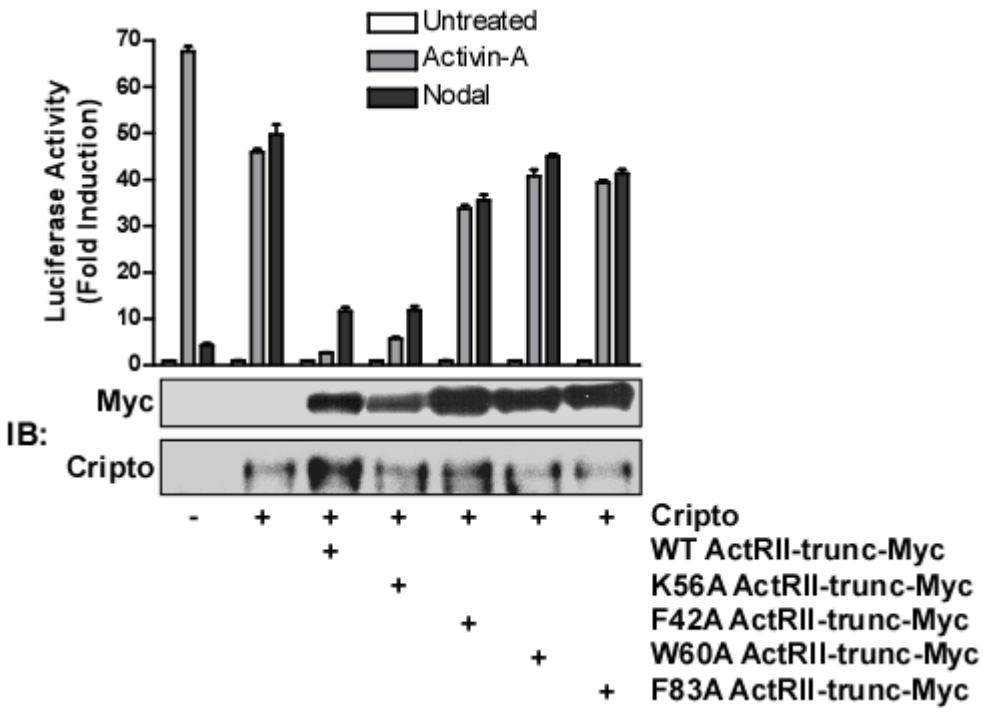

Figure 5: Nodal and activin-A bind the same site on ActRII. 293T cells were transfected with A3-lux, FAST2 and CMV-β-galactosidase together with 200 ng of empty vector or Cripto and 200 ng of ActRII-trunc constructs as indicated. Cells were treated with 100 pM activin-A or 30 nM Nodal as indicated and resulting normalized luciferase activities are presented as fold induction. Corresponding cell lysates were subjected to Western blotting using anti-Myc or anti-Cripto antibodies as described under Experimental Procedures.

Truncated ALK4 mutants with disrupted activin-A binding retain the ability to bind Cripto. Nodal forms signaling complexes that contain Cripto, ActRII and ALK4 and in these complexes ALK4 is thought to form distinct contacts with Cripto and Nodal (Yeo and Whitman, 2001). Here we have tested whether ALK4 also has distinct and separable binding sites for Cripto and activin-A. Similar to ActRII-trunc, membrane-anchored, kinase-deleted ALK4 (ALK4-trunc) inhibits activin-A signaling by forming non-productive complexes with ActRII and activin-A (Tsuchida et al., 1995). We previously used

alanine substitution mutagenesis to identify a cluster of three amino acid residues on the ALK4-ECD that are each required for the dominant negative function of ALK4-trunc (Harrison et al., 2003). These residues, Ile^{70}, Leu^{75} and Pro^{77} were subsequently shown to be required for activin-A binding as well as for ALK4 signaling function (Harrison et al., 2003). Since the binding sites on ALK4 for Nodal and Cripto are thought to be distinct, we reasoned that ALK4-trunc mutants with disrupted activin-A binding might retain their ability to bind Cripto.

To test this, we transfected 293T cells with untagged WT Cripto or ΔCFC Cripto in the absence or presence of Flag-tagged WT ALK4-trunc, L75A ALK4-trunc, P77A ALK4-trunc or I70A ALK4-trunc. Cell lysates were then subjected to anti-Flag immunoprecipitation followed by Western blot using anti-Cripto or anti-Flag antibodies. As predicted, WT Cripto co-precipitated with WT ALK4-trunc while ΔCFC did not (Figure 6). Importantly, the L75A, P77A and I70A ALK4-trunc proteins each co-precipitated with WT Cripto but not with ΔCFC indicating these ALK4 mutations do not affect Cripto-ALK4 binding. This result demonstrates that ALK4 has distinct and separable binding sites for activin-A and Cripto and it is consistent with our conclusions drawn from data presented above that activin-A and Nodal can form structurally and functionally similar receptor complexes containing Cripto.

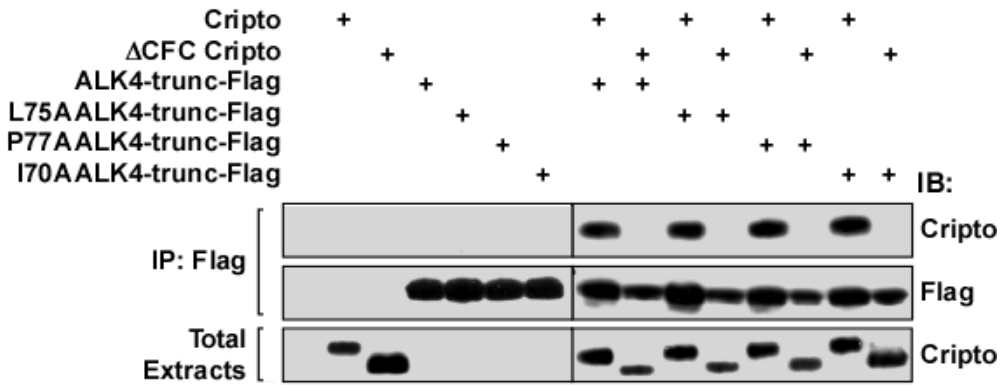

Figure 6: Kinase-deleted ALK4 (ALK4-trunc) mutants with disrupted activin-A binding retain Cripto binding. 293T cells were transfected with indicated Cripto and/or of Flag-tagged ALK4-trunc constructs with resulting cell lysates subjected to anti-Flag immunoprecipitation followed by Western blotting using anti-Cripto or anti-Flag antibodies. Alternatively, total cell extracts were subjected to Western blotting using and anti-Cripto antibody as described under Experimental Procedures.

ALK4-trunc mutants antagonize the opposing effects of Cripto on activin-A- and Nodal-dependent luciferase induction. Since these ALK4-trunc mutants, deficient in activin binding, retain the ability to bind Cripto, we hypothesized that they might sequester Cripto away from ligand/receptor complexes thereby reducing Nodal signaling on the one hand while increasing activin-A signaling on the other. To test this possibility, we asked whether these ALK4-trunc mutants could target Cripto function. 293T cells were transfected with empty vector, Cripto, ALK4-trunc or L75A ALK4-trunc as indicated. As shown in Figure 7A, L75A ALK4-trunc had no effect on activin-A signaling in the absence of Cripto but was able to block Cripto antagonism of activin-A signaling in a dose dependent manner. Conversely, as shown in Figure 7B, increasing amounts of L75A ALK4-trunc DNA caused a dose-dependent decrease in Cripto-

dependent Nodal signaling. However, the highest DNA dose of the L75A ALK4-trunc construct only blocked Nodal signaling by ~50%. This may be explained by our observation that Nodal signaling can be facilitated by very low levels of transfected Cripto DNA as well as by the fact that Cripto is overexpressed in this experiment. Therefore, we predict that a high DNA ratio of L75A ALK4-trunc to Cripto may be required to see complete block of Nodal signaling in this assay. As expected, the I70A and P77A ALK4-trunc mutants possess similar Cripto-blocking capability (data not shown).

In order to ensure that the progressive loss of Cripto function was due to the presence of L75A ALK4-trunc protein and not the result of a decrease in Cripto expression, we measured the levels of these proteins at the cell surface. Figure 7C shows that the level of cell surface L75A ALK4-trunc expression correlated with the amount of DNA transfected and, importantly, that its expression did not cause the cell surface levels of Cripto to decrease. Finally, we have performed Western blots on total cell lysates from 293T cells transfected with an equal molar ratio of Cripto and L75A ALK4-trunc DNA under condition that resulted in a blockade of Cripto function. As shown in Figure 7D, the expression levels of these proteins are unaffected by their co-expression. Therefore, in summary, we have shown that the L75A ALK4-trunc mutant binds Cripto and also

prevents Cripto effects on Nodal- and activin-A-induced luciferase expression.

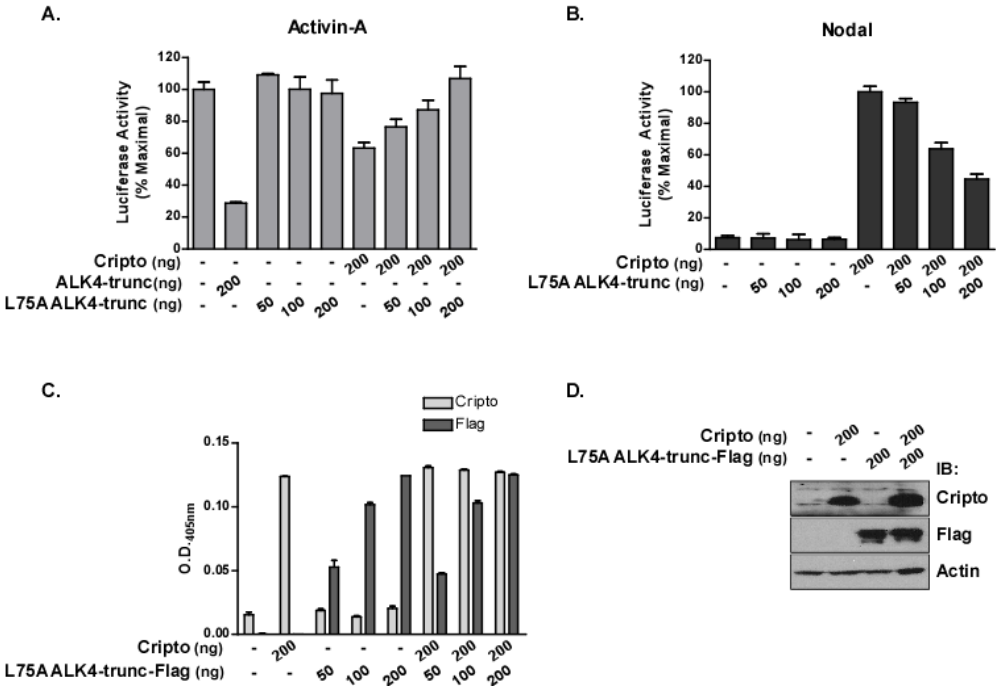

Figure 7: ALK4-trunc L75A blocks Cripto effects on Nodal and activin-A signaling in a dose-dependent manner. 293T cells were transfected with empty vector or Cripto DNA in the absence or presence of wild type ALK4-trunc or the indicated doses of L75A ALK4-trunc DNA together with A3-lux, FAST2 and CMV-β-galactosidase constructs as described under Experimental Procedures. Cells were treated with 250 pM activin-A (A) or 10 nM Nodal (B) and resulting luciferase activities were normalized relative to β-galactosidase activities and are presented as % maximal induction. (C) Cell surface expression of Cripto and L75A ALK4-trunc was measured using an intact cell ELISA assay as described under Experimental Procedures. (D) Cripto and L75A ALK4-trunc constructs were transfected into 293T cells at an equimolar DNA ratio and then resulting cell lysates were subjected to Western blotting using anti-Cripto, anti-Flag, or anti-Actin antibodies as described under Experimental Procedures.

Activin-A and Nodal form analogous receptor complexes with Cripto via distinct assembly mechanisms. In the absence of Cripto, activin-A forms high potency, high efficacy signaling complexes with ActRII and ALK4. Conversely, Nodal is incapable of signaling in the absence of Cripto (Figure 8A). The data presented

here support a model in which activin-A and Nodal each form similar signaling complexes that contain Cripto (Figure 8B). According to this model, activin-A first binds its type II receptors with high affinity and then recruits ALK4 and Cripto into high potency, low efficacy complexes. On the other hand, Nodal first binds Cripto before it can assemble ActRII/IIB and ALK4 into low potency, low efficacy complexes. Figure 8C schematically outlines how the level of Cripto impacts Nodal and activin signaling. In the absence of Cripto (Figure 8C, *a*), activin forms only high efficacy signaling complexes while Nodal is unable to signal. As the level of Cripto increases, activin signaling decreases and Nodal signaling increases until they converge (Figure 8C, *b*). At this point, all receptor complexes contain Cripto and therefore have low efficacy. Finally, as shown in Figure 8D, ALK4-trunc mutants deficient in activin-A binding retain the ability to bind Cripto and block its ability to form signaling complexes with activin-A and Nodal.

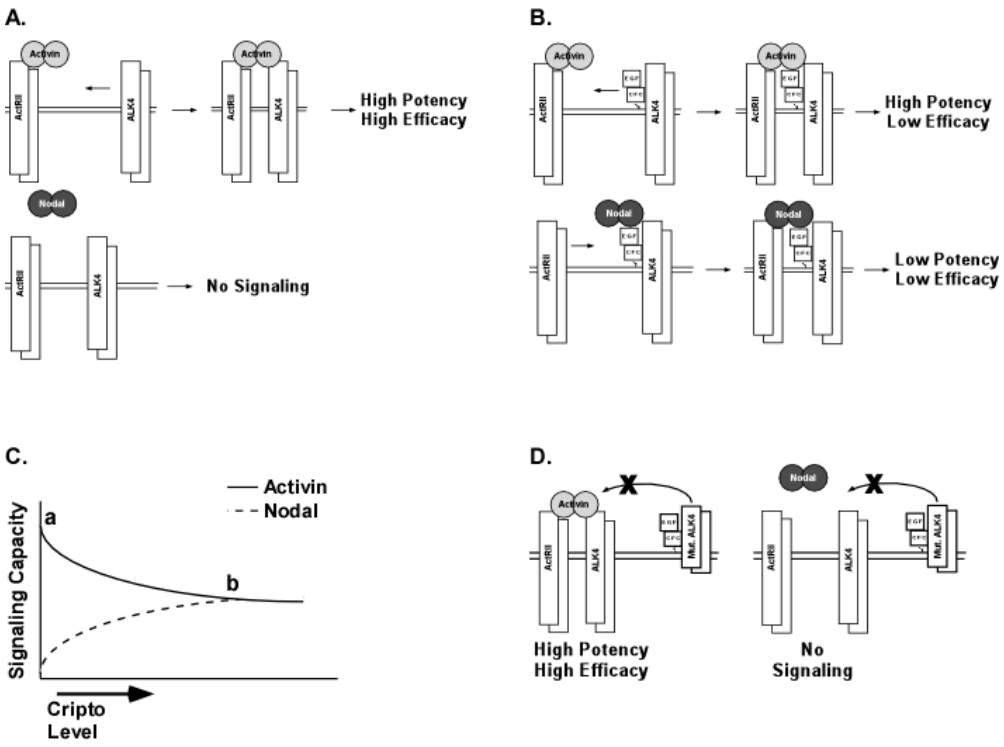

Figure 8: Cripto reduces activin-A efficacy to a level similar to that of Nodal and forms similar signaling complexes with both ligands. (A) In the absence of Cripto, activin-A forms high potency, high efficacy signaling complexes with ActRII/IIB and ALK4 while Nodal does not bind these receptors or initiate signaling. (B) When Cripto is present, activin-A and Nodal each form structurally similar signaling complexes that contain Cripto. Activin-A first binds its type II receptors with high affinity and then recruits ALK4 and Cripto into a high potency, low efficacy complex. Nodal first binds Cripto before it can assemble ActRII/IIB and ALK4 into a low potency, low efficacy complex. (C) Diagram illustrating the ability of Cripto to modulate activin and Nodal signaling in a dose-dependent manner. In the absence of Cripto activin signaling is high while Nodal does not signal (*a*). As Cripto levels increase, activin signaling decreases and Nodal signaling increases until they converge (*b*). (D) ALK4-trunc mutants deficient in activin-A binding retain the ability to bind Cripto and block its ability to form signaling complexes with activin-A and Nodal.

DISCUSSION

TGF-β ligands are morphogens that regulate gene expression and specify cell fate in a concentration dependent manner (McDowell and Gurdon, 1999; Schmierer and Hill, 2007). However, Smad proteins are the central mediators of TGF-β signaling and therefore the magnitude and duration of the Smad response are critical in

determining patterns of gene expression. Importantly, Smad signaling is shaped not only by the concentration of TGF-β ligands but also by an array of cell- and ligand-specific modulators that operate through multiple mechanisms (Schmierer and Hill, 2007; Shi and Massague, 2003). Cripto is one such modulator that affects the signaling of several TGF-β ligands that activate the Smad2/3 pathway. These include Nodal (Schier, 2003), GDF1 (Cheng et al., 2003), GDF3 (Chen et al., 2006), activin-A (Gray et al., 2003), activin-B (Adkins et al., 2003) and TGF-β1 (Gray et al., 2006). Interestingly, while Cripto functions as an obligatory co-receptor for Nodal, GDF1 and GDF3, it antagonizes signaling by activin-A, activin-B and TGF-β1. Therefore, by altering its level of Cripto expression, a cell can tune its responsiveness to these ligands and vary its level of Smad2/3 signaling over a broad range.

In the present study we conducted a detailed comparison of the roles of Cripto as a modulator of activin and Nodal signaling. In contrast to previous reports exclusively postulating that Cripto inhibits activin signaling by forming inactive complexes with activin and/or its receptors, our data support a novel mechanism whereby Cripto participates in functional activin signaling complexes that have reduced signaling capacity. We conclude that Cripto is a non-competitive activin antagonist since it reduced activin efficacy without altering activin potency (EC_{50}). Also, its maximal inhibitory effect on activin signaling was partial and attained at sub-maximal Cripto expression levels. In

light of these findings, we propose that activin receptor complexes can exist in two signaling states, a high efficacy state in the absence of Cripto (Figure 8A and 8C,a) and a lower efficacy state in the presence of Cripto (Figure 8B and 8C,b). According to this model, Nodal and other ligands that require Cripto can only signal in the low efficacy state. Activins on the other hand signal in the high efficacy state when Cripto is absent and in the low efficacy state when Cripto is present.

This two state model of activin receptor signaling is supported by our discovery that the maximal signaling responses to activin and Nodal converge as the level of Cripto expression increases. Specifically, Cripto reduced activin-A-dependent luciferase induction and Smad2 phosphorylation to levels indistinguishable from those induced by Nodal. In each of these assays, we found that activin-A and Nodal had similar response maxima in cells expressing high levels of Cripto. However, while Cripto effectively converted activin-A into a partial agonist with efficacy resembling that of Nodal, it did not alter activin-A potency indicating that Cripto does not affect the affinity of activin-A for ActRII/IIB. In this regard, we found that activin-A was nearly 250 times more potent than Nodal, suggesting that the affinity of activin-A for ActRII/IIB is much higher than that of Nodal for Cripto, although this remains to be tested directly. In summary, we propose that activin and Nodal form functionally similar signaling complexes in

the presence of Cripto despite the fact that these ligands have distinctly different mechanisms of receptor assembly.

Our results demonstrate that activin can elicit a substantially larger signaling response in the absence of Cripto than Nodal can generate in the presence of Cripto. This finding predicts that Nodal will be unable to regulate the expression of certain activin-responsive genes that require high levels of Smad2/3 signaling. On the other hand, our results show that activin and Nodal signaling responses converge in the presence of Cripto and therefore also predict that activin and Nodal will elicit similar biological effects on cells that express Cripto. Notably, these predictions appear to be supported by the demonstration that activin-B and Xenopus Nodal related proteins (Xnrs) regulate the expression of disparate sets of genes during Xenopus embryogenesis, with activin-B affecting the expression of nearly twice as many genes as Xnrs (Ramis et al., 2007). In addition to cooperating with Xnrs to regulate developmental genes such as goosecoid, chordin, Xbra, Xnr2 and Derrière (Piepenburg et al., 2004), Ramis *et al.* showed that activin-B exclusively regulated the expression of several genes involved in cell cycle control consistent with its antiproliferative role during gastrulation. In this regard, it is interesting to note that Smad2/3-mediated antiproliferative effects have previously been reported to require high, sustained levels of Smad2/3 signaling (Nicolas and Hill, 2003). Therefore, high efficacy activin signaling may

be required to induce growth arrest during *Xenopus* gastrulation while lower efficacy activin and Xnrs signaling in the presence of *Xenopus* Cripto proteins may cooperate to control mesodermal patterning. Importantly, these studies appear to be consistent with our observation that the intrinsic efficacy of activin-A is greater than that of Nodal but that these ligands signal similarly in the presence of Cripto. Further studies will be necessary to determine how Cripto expression levels shape gene transcription responses to activin and Nodal ligands.

The similar efficacies of activin and Nodal in the presence of Cripto suggested that these ligands assemble Cripto-containing signaling complexes that are structurally similar. In support of this, we provide biochemical evidence for complexes containing activin-A, Cripto and both receptor types and show that the assembly of such complexes is competitively inhibited by Nodal. We further demonstrate that Nodal and activin-A share the same binding site on ActRII. This result was somewhat surprising since Nodal, unlike activin, requires Cripto to bind type II receptors (Yeo and Whitman, 2001). Notably, activin residues that mediate type II receptor binding are not conserved in Nodal and substitution of a 14 amino acid ActRII-binding region from activin into Nodal resulted in a chimera that could signal in a Cripto-independent manner (Cheng et al., 2004). Despite these differences in their type II receptor binding properties, however, our results clearly demonstrate that activin-A and Nodal bind the same residues on

ActRII. We have also shown that ALK4 has distinct and separable binding sites for activin-A and Cripto. This result supports our observation that ALK4 and Cripto are both present in complexes together with activin-A and ActRII and is also consistent with our conclusion that activin-A and Nodal form similar receptor complexes in the presence of Cripto. Together, these results indicate that despite their differing mechanisms of receptor assembly, Nodal and activin form structurally similar complexes with Cripto and activin type I and type II receptors.

While our data indicate that Cripto is present in activin receptor complexes, they do not address the question of how the presence of Cripto in these signaling complexes reduces activin efficacy. We propose two possible models. First, although we show that Cripto does not preclude ALK4 recruitment into activin signaling complexes as was previously proposed (Gray et al., 2003), it is possible that ActRII-bound activin has lower affinity for Cripto-bound ALK4 than it has for ALK4 alone. Therefore, by reducing the affinity of activin for ALK4, Cripto could reduce the stability of activin signaling complexes and thereby reduce signaling. Such a mechanism is consistent with our observation here and previously (Gray et al., 2003) that Cripto reduces activin crosslinking to ALK4. Alternatively, Cripto may act as a wedge that distorts signaling complexes in a way that limits the ability of the ActRII kinase to phosphorylate ALK4 or the ability of ALK4 to phosphorylate

Smads or both. Biochemically, these spatial constraints may explain the observed decrease in the efficiency of crosslinking between activin and ALK4 in the presence of Cripto. Such a model postulates that Cripto imposes similar structure/function constraints on signaling complexes assembled by either activin-A or Nodal and is therefore appealing since it can explain our observation that activin-A and Nodal attain similar signaling maxima in the presence of Cripto. Three-dimensional structures of complexes containing activin or Nodal, their receptors and Cripto will allow a comparison with similar structures that have been solved in the absence of Cripto (Allendorph et al., 2006; Greenwald et al., 2004; Thompson et al., 2003) and will provide further insight into the structural basis for the effects of Cripto on signaling complexes containing ActRII/IIB and ALK4. According to this revised model, we predict that the three-dimensional structures of activin and Nodal in complex with Cripto and their receptors will be very similar.

We have shown here that three ALK4-trunc mutants each lacking activin binding were indistinguishable from WT ALK4-trunc in their ability to bind Cripto. This finding indicates that ALK4 has distinct and separable binding sites for activin and Cripto. We have further demonstrated that these ALK4-trunc mutants inhibit Cripto-dependent effects on activin and Nodal signaling, as illustrated by the L75A ALK4-trunc mutant. The effects of this mutant were dose-dependent and apparently stemmed from its ability to bind Cripto and sequester it

away from ligand/receptor complexes (Figure 8D). However, future studies will be required in order to elucidate the precise mechanism by which these ALK4 mutants inhibit specific Cripto functions.

In addition to supporting our model in which Cripto mediates activin and Nodal signaling by forming similar signaling complexes with these ligands, the ability of these ALK4-trunc mutants to block Cripto effects on activin and Nodal signaling suggests that they may have therapeutic value as Cripto inhibitors. For example, Cripto has been identified as a marker of stem cell pluripotency (Adewumi et al., 2007) and it has been shown that ES cells lacking Cripto spontaneously differentiate into neurons (Parish et al., 2005; Parisi et al., 2003; Xu et al., 1998). Therefore, developing a Cripto-blocking reagent such as L75A ALK4-trunc may aid efforts aimed at providing cell-based treatments for neurodegenerative disorders. Cripto is also highly expressed in human tumors and is thought to promote tumorigenesis via multiple mechanisms (Strizzi et al., 2005) including antagonism of activin (Adkins et al., 2003; Gray et al., 2003) and TGF-β (Gray et al., 2006)signaling as well as facilitation of Nodal signaling (Topczewska et al., 2006). Therefore, these ALK4-trunc mutants may also have utility as cancer therapeutic agents.

In summary, the results presented here provide a molecular mechanism that explains the basis for the opposing effects of Cripto on activin and Nodal signaling. We have shown for the first time that the

intrinsic efficacy of activin is higher than that of Nodal and we have further demonstrated that Cripto forms reduced efficacy complexes with activin and its receptors that structurally and functionally resemble Nodal signaling complexes. Thus, our results reconcile the opposing effects of Cripto on Nodal and activin signaling and suggest a model in which Cripto participates in similar signaling complexes with each ligand.

Chapter 1, in full, contains text and data published in the Journal of Biological Chemistry, 2008 Feb 22;283(8):4490-500 (with Shani G, Booker EC, Vale WW, Gray PC). The disseratation author was the primary investigator and author of this report.

CHAPTER 2

BLOCKADE OF CRIPTO BINDING TO CELL SURFACE GRP78 INHIBITS ONCOGENIC CRIPTO SIGNALING VIA MAPK/PI3K AND SMAD2/3 PATHWAYS

INTRODUCTION

Cripto (Cripto-1, TDGF1) is an extracellular, GPI-anchored signaling protein with important roles during embryonic development, stem cell function and cancer progression (Adewumi et al., 2007; Strizzi et al., 2005). While Cripto expression is generally low or absent in normal adult tissues, it is found at high levels in many human tumors and its overexpression promotes various tumorigenic attributes including cellular proliferation, migration and epithelial-to-mesenchymal transition (EMT) (Strizzi et al., 2005). Cripto transgenic mice were shown to develop mammary tumors (Strizzi et al., 2004; Wechselberger et al., 2005) and monoclonal antibodies targeting Cripto reduced the growth of tumor xenografts in nude mice (Adkins et al., 2003; Xing et al., 2004).

Cripto exerts its biological effects by modulating the signaling of TGF-β superfamily members and activating MAPK/PI3K pathways. TGF-β ligand-induced assembly of serine/threonine kinase transmembrane receptors (type I and type II) triggers activation of the

type I receptor kinase which phosphorylates cytoplasmic Smad proteins causing them to translocate to the nucleus where they regulate transcription of target genes (Shi and Massague, 2003). Cripto can bind to type I receptors, ALK4 (Yeo and Whitman, 2001) and ALK7 (Reissmann et al., 2001), and is an obligatory co-receptor for certain TGF-β ligands such as Nodal (Shen, 2007). Cripto co-receptor function is essential during embryogenesis (Strizzi et al., 2005) and it has also been implicated in promoting tumor growth since Nodal signaling was recently shown to play a key role in promoting tumorigenicity of human melanoma and breast cancer cells (Postovit et al., 2008; Topczewska et al., 2006). In contrast to its role as a Nodal co-receptor, Cripto inhibits activin signaling (Adkins et al., 2003; Gray et al., 2003; Kelber et al., 2008) and cytostatic TGF-β1 effects (Gray et al., 2006; Shani et al., 2008; Shukla et al., 2008). Soluble forms of Cripto also activate ras/raf/MAPK and PI3K/Akt pathways via c-Src leading to the designation of Cripto as tumor growth factor (Bianco et al., 2003; Strizzi et al., 2005). The extracellular proteoglycan glypican-1 was shown to be required for this Cripto tumor growth factor activity (Bianco et al., 2003) but the receptor mechanism involved remains to be fully explored. Interestingly, this pathway was also shown to be independent of ALK4 and Nodal (Bianco et al., 2002), suggesting that Cripto regulates Smad2/3 and MAPK/PI3K pathways via non-overlapping mechanisms.

In an effort to further characterize Cripto signaling, we recently conducted a screen aimed at identifying novel Cripto binding proteins. This led to the identification of Glucose Regulated Protein-78 (GRP78), an ER chaperone in the heat shock protein 70 (HSP70) family that is highly expressed in tumors and that promotes tumor cell survival, chemoresistance and malignancy (Dong et al., 2008; Lee, 2007). Notably, GRP78 is localized to the plasma membrane of tumor cells where it has receptor-like functions associated with increased cellular proliferation, motility and survival (Misra et al., 2006; Misra et al., 2004; Philippova et al., 2008). Here, we now demonstrate that Cripto binding to cell surface GRP78 is a necessary upstream event that mediates Cripto signaling via both MAPK/PI3K and Smad2/3 pathways. Importantly, blockade of this interaction precludes oncogenic Cripto effects, including increased cell proliferation, downregulation of E-Cadherin, decreased cell adhesion and promotion of pro-proliferative responses to activin-A and Nodal.

MATERIALS AND METHODS

Materials. NuPAGE gels, molecular weight markers, and the CyQUANT cell proliferation and adhesion assay kit were obtained from Invitrogen (San Diego, CA). Recombinant human activin-A was generated using a stable activin-A-expressing cell line generously provided by Dr. J. Mather (Genentech, Inc.) and was purified by Wolfgang Fischer (Peptide Biology Laboratory, Salk institute).

Recombinant mouse Nodal, human TGF-β1, human activin-B, mouse Cripto, and anti-E-Cadherin (1:500) were purchased from R&D Systems (Minneapolis, MN). Protein A- and G-agarose and the PI3K (LY294002) and MEK kinase (PD98059) inhibitors were purchased from Calbiochem (San Diego, CA). ^{125}I-Cripto was prepared using the chloramine T method as described previously (Vaughan JM 1993 Endocrinology). Polyclonal anti-Cripto antibody (6900) was previously described and used at a 1:500 dilution (Shani et al., 2008). Goat IgG, anti-GRP78 (N-20) and anti-phospho-tyrosine (PY99) were purchased from Santa Cruz Biotechnology, Inc. (Santa Cruz, CA) and used at 1:200 dilution for Western blots. Anti-phospho-Smad2 (1:500), anti-Smad2/3 (1:500), anti-pan-actin (1:1000), anti-phospho-Akt (1:500), anti-Akt (1:500), anti-phospho-Erk1/2 (1:500), anti-Erk1/2 (1:200), anti-phospho-Src (Y416) (1:500), and anti-Src (1:500) were purchased from Cell Signaling Technologies, Inc. (Danvers, MA). Anti-HA (1:200), anti-M2 Flag (1:500) and anti-Flag (M2) agarose were purchased from Sigma (St. Louis, MO). Horseradish peroxidase-linked anti-mouse (1:10000), anti-goat (1:10000), anti-rabbit IgG (1:10000), 3,3',5'5-tetramethlbenzidine substrate, chemiluminescent substrate (Supersignal^{TM}), and the BCA protein assay kit were obtained from Pierce (Rockford, IL).

Expression constructs. The wild-type Cripto-Flag expression constructs have previously been described (Gray et al., 2006). GRP78-

HA and Δ19-68 GRP78-HA constructs were made using standard PCR techniques (Harrison et al., 2003). The lentiviral expression (Miyoshi et al., 1998) and shRNA (Singer et al., 2005) vectors for Cripto (Gray et al., 2006) and GRP78 (Shani et al., 2008) have been previously described.

Cell Lines, Transfection and Infection. HEK 293T cells and NCCIT cells were cultured as recommended by American Type Culture Collection (ATCC). MCF10A cells were cultured as previously described (Debnath et al., 2003). H9 (WiCell Inc., Madison, Wisconsin, USA) human embryonic stem cells were maintained in defined mTeSR-1 media (StemCell Technologies, Vancouver, BC, Canada) on growth-factor-depleted matrigel (BD Biosciences, San Jose, CA) coated plates. NCCIT cells and 293T cells were transfected with Lipofectamine 2000 (Invitrogen) and Perfectin (Gene Therapy Systems), respectively, according to manufacturer's instructions. Lentivirus was produced as previously described (Miyoshi et al., 1998). Cells were infected as previously described (Gray et al., 2006).

Detection of Cell Surface Proteins. Protein detection via intact cell surface ELISA was performed as previously described (Gray et al., 2000).

Immunoprecipitation and Western blotting. Phosphoprotein analysis was essentially carried out as previously described (Kelber et al., 2008). Cells were grown to confluence in 24-well plates, rinsed with

serum-free media and serum-starved for 4 hours. Appropriate inhibitors or blocking antibodies were added as indicated for 1 hour. Following growth factor treatment, cells were harvested and lysates were analyzed by Western blot. Co-immunoprecipitation studies were carried out as previously described (Kelber et al., 2008).

Luciferase Assays. Luciferase assays were carried out in NCCIT cells using the A3-luciferase reporter as previously described (Gray et al., 2003).

Confocal Microscopy. H9 cells were cultured on matrigel-coated coverslips. Cells were first blocked in 5%FCS/PBS (buffer A) at room temperature for 15-30 min, and then stained in buffer A containing rabbit anti-Cripto (6900), goat anti-GRP78 (N-20, Santa Cruz Biotechnology, Santa Cruz, CA), and mouse anti-E-cadherin (36/E-Cadherin, BD Biosciences, San Jose, CA) at 10^0C for 30 min. Following washing, cells were stained with anti-rabbit, anti-goat, and anti-mouse fluorescently-conjugated secondary antibodies in buffer A at 10^0C for 30 min. Cells were washed and fixed with 4% paraformaldehyde at room temperature for 15 min. Coverslips were then mounted in the presence of DAPI (4', 6'-diamidino-2-phenylindole), and analzed by confocal microscopy using a Leica TCS SP2 AOBS confocal microscope (Leica, Wetzlar, Germany). Sequential scanning of each excited wavelength was utilized to prevent bleed-through between fluorochromes in analysis.

Cell Proliferation Assays. The Invitrogen CyQUANT Cell Proliferation kit was used according to the manufacturer's protocol. Cells were plated on 96-well plates at a density of 500 (NCCIT) or 200 (MCF10A) cells/well. 24 hours later, cells were either treated with indicated combinations of blocking agents (goat IgG or anti-GRP78 (N-20)) and growth factors or left untreated in quadruplicate. Cell growth was measured eight days later.

Cripto Binding Assays. ^{125}I-Cripto binding to the cell surface of NCCIT and MCF10A cells was carried out essentially as previously described (Harrison et al., 2004).

E-Cadherin Expression and Cell Adhesion. MCF10A cells were plated at $4x10^5$ cells/well in 6-well plates. 24 hours later cells were pretreated with goat IgG or anti-GRP78 (N-20) for 1 hour and then treated with 400 ng/ml soluble Cripto or left untreated. 48 hours after treatment, cell lysates were analyzed by Western blot, as described above. Cells were also analyzed for their adhesive properties using the Invitrogen CyQUANT Prolifertion kit, as recommended by the manufacturer.

RESULTS

Cripto and GRP78 cooperatively regulate activin/Nodal/TGF-β signaling. Cell lines derived from germ cell tumors, including mouse P19, human NTera2 and human NCCIT, are developmentally pluripotent and resemble embryonic stem cells (Yu

and Thomson, 2008). Like ES cells, these embryonal carcinoma (EC) cell lines express relatively high levels of Cripto making them useful for characterizing endogenous Cripto functions. In order to test the functional interaction between Cripto and GRP78, we generated NCCIT cell populations stably expressing shRNAs targeting Cripto and/or GRP78. These shRNAs reduced levels of Cripto and/or GRP78 protein in total cell lysates (Figure 9A) and at the cell surface (Figure 9B). Importantly, shRNA knockdown of Cripto did not significantly affect cell surface levels of GRP78 and vice versa (Figure 9B).

Activins, Nodal and TGF-βs each signal via Smad2 and Smad3 (Shi and Massague, 2003) and we used these NCCIT cells expressing Cripto and/or GRP78 shRNAs to test whether GRP78 plays a role in Cripto regulation of activin-A- and Nodal-induced Smad2 phosphorylation. As shown in Figure 9C, activin-A-induced Smad2 phosphorylation was enhanced in cells with reduced Cripto expression consistent with our previous demonstration that Cripto inhibits activin-A signaling (Gray et al., 2003; Kelber et al., 2008). Interestingly, Activin-A-dependent Smad2 phosphorylation was similarly increased in GRP78 knockdown cells and also in cells with both Cripto and GRP78 knocked down (Figure 9C). By contrast to its effects on activin-A signaling, knockdown of Cripto reduced Nodal-dependent Smad2 phosphorylation as expected (Figure 9D). While knockdown of GRP78 alone also appeared to cause a modest inhibition of Nodal signaling,

knockdown of Cripto and GRP78 together inhibited Nodal signaling to a greater extent than knockdown of either protein alone (Figure 9D). Together, these data are consistent with a cooperative role for Cripto and GRP78 in causing opposing effects on activin-A and Nodal signaling.

We used the same shRNA-expressing NCCIT cells to test the effects of GRP78 knockdown on Cripto regulation of TGF-β1, Nodal, activin-A, and activin-B signaling as measured by their induction of a Smad2-responsive luciferase reporter construct. As shown in Figure 9E, shRNA knockdown of either Cripto or GRP78 expression caused a modest but significant increase in activin-A, activin-B and TGF-β1 signaling. By contrast, shRNA knockdown of Cripto significantly decreased Nodal signaling. Notably, knockdown of Cripto and GRP78 together caused activin-A, activin-B and TGF-β1 signaling to be further enhanced while Nodal signaling was undetectable (Figure 9E). Nodal-dependent luciferase induction was relatively weak in NCCIT cells and we were unable to observe an effect of GRP78 knockdown (Figure 9E). Therefore, we used the same Smad2-dependent reporter system in 293T cells that express cell surface GRP78 (Shani et al., 2008) but lack endogenous Cripto (Yan et al., 2002). As shown in Figure 9F, Nodal signaling in 293T cells was completely dependent on exogenous Cripto and Cripto-dependent Nodal signaling was enhanced in the presence of overexpressed GRP78. Furthermore, as shown in Figure

9G, Cripto-dependent Nodal signaling was attenuated in these cells when endogenous GRP78 was knocked down. Together, these results support a role for GRP78 as a mediator of Cripto signaling via activin/Nodal/TGF-β ligands in embryonal carcinoma cells.

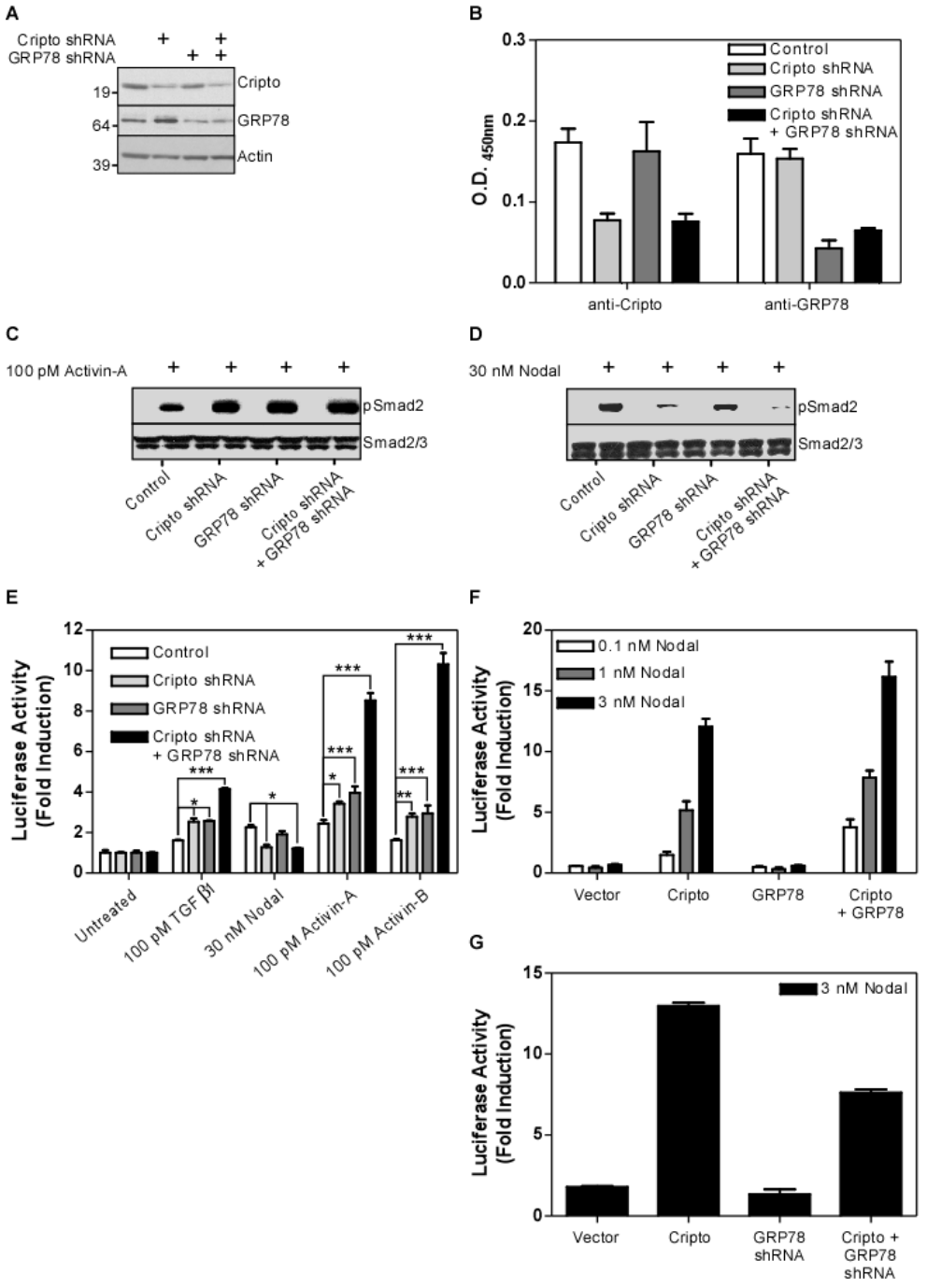

Figure 9. Cripto and GRP78 cooperatively regulate activin/Nodal/TGF-β signaling. NCCIT cells stably expressing Cripto and/or GRP78 shRNAs were analyzed by Western blot (A) or intact cell surface ELISA (B) using the indicated antibodies. The same cells were treated with activin-A (C) or Nodal (D) and resulting levels of phospho-Smad2 (pSmad2) and Smad2 were measured by Western blot using pSmad2 and Smad2 antibodies. NCCIT cells (E) and 293T cells (F, G) overexpressing the indicated proteins and/or shRNAs were transfected with a Smad2-responsive luciferase reporter and treated with the indicated doses of TGF-β ligands. Resulting luciferase activities were normalized and are presented as fold induction over untreated samples.

Antibody blockade of cell surface GRP78 inhibits Cripto signaling via TGF-β ligands in hEC and hES cells. The antibody we used to detect cell surface GRP78 (N-20, Santa Cruz) has previously been shown to block cell surface GRP78 receptor function (Davidson et al., 2005; Philippova et al., 2008). This antibody binds cell surface GRP78 in NCCIT cells (Figure 9B) and we tested whether it blocks Cripto signaling via activin/Nodal/TGF-β ligands in these cells. As shown in Figure 10A, treatment of NCCIT control cells with the N-20 antibody increased activin-A, activin-B and TGF-β1 signaling and decreased Nodal signaling similar to what was observed following Cripto knockdown in these cells (Figure 9E). Importantly, N-20 antibody treatment did not significantly affect activin-A, activin-B, Nodal or TGF-β1 signaling in Cripto knockdown cells (Figure 10B) indicating that the antibody exerts its effects on these ligands by blocking Cripto function. Together, these results suggest that cell surface GRP78 is required for Cripto-dependent regulation of activin/Nodal/TGF-β signaling.

Since the N-20 antibody inhibits Cripto signaling, our results raise the possibility that Cripto and the N-20 antibody compete for binding to GRP78. This antibody targets an epitope within the first 50 amino acids of GRP78 and we generated a GRP78 mutant (Δ19-68 GRP78) lacking this region and tested its ability to bind Cripto. Figure 10C illustrates the position of the N-20 epitope and the Δ19-68 GRP78

mutant in which it is deleted. When lysates from 293T cells overexpressing these proteins were subjected to immunoprecipitation with an HA antibody followed by Western blot using N-20 or HA antibody, the N-20 antibody detected wild type GRP78 but not the Δ19-68 GRP78 mutant in which the N-20 epitope was deleted (Figure 10D). Importantly, as shown in Figure 10E, wild type GRP78 co-immunoprecipitated with Cripto but the Δ19-68 GRP78 mutant did not. This result indicates that the N-20 antibody and Cripto share a binding site on GRP78 and suggests that they may compete for GRP78 binding.

Cripto is expressed in embryonic stem cells where it has been shown to have key roles in regulating differentiation and pluripotency (Minchiotti, 2005). We tested whether GRP78 co-localizes with Cripto and regulates Cripto function in hES cells. As shown in Figure 10F, GRP78 and Cripto are both expressed at the surface of H9 hES cells as measured by cell surface ELISA. Next, we subjected H9 hES cells to cell surface immunostaining with Cripto, GRP78 and E-Cadherin antibodies to test whether these proteins co-localize at the plasma membrane. As shown in Figure 10G, Cripto and GRP78 each displayed punctate staining and their staining patterns overlapped with that of E-Cadherin, a cell surface marker. Importantly, Cripto and GRP78 also displayed a partially overlapping staining pattern with each other indicating that they co-localize at the cell surface (Figure 10G).

Finally, we tested whether immunoneutralization of cell surface GRP78 affects Cripto modulation of activin-A and Nodal signaling in hES cells. Indeed, as shown in Figure 10H, treatment of H9 hES cells with the N-20 GRP78 antibody increased Smad2 phosphorylation in response to activin-A and decreased Smad2 phosphorylation in response to Nodal. Together, these results demonstrate that targeting cell surface GRP78 disrupts Cripto effects on TGF-β ligand signaling and provide the first evidence of a functional cell surface Cripto/GRP78 complex in hESCs.

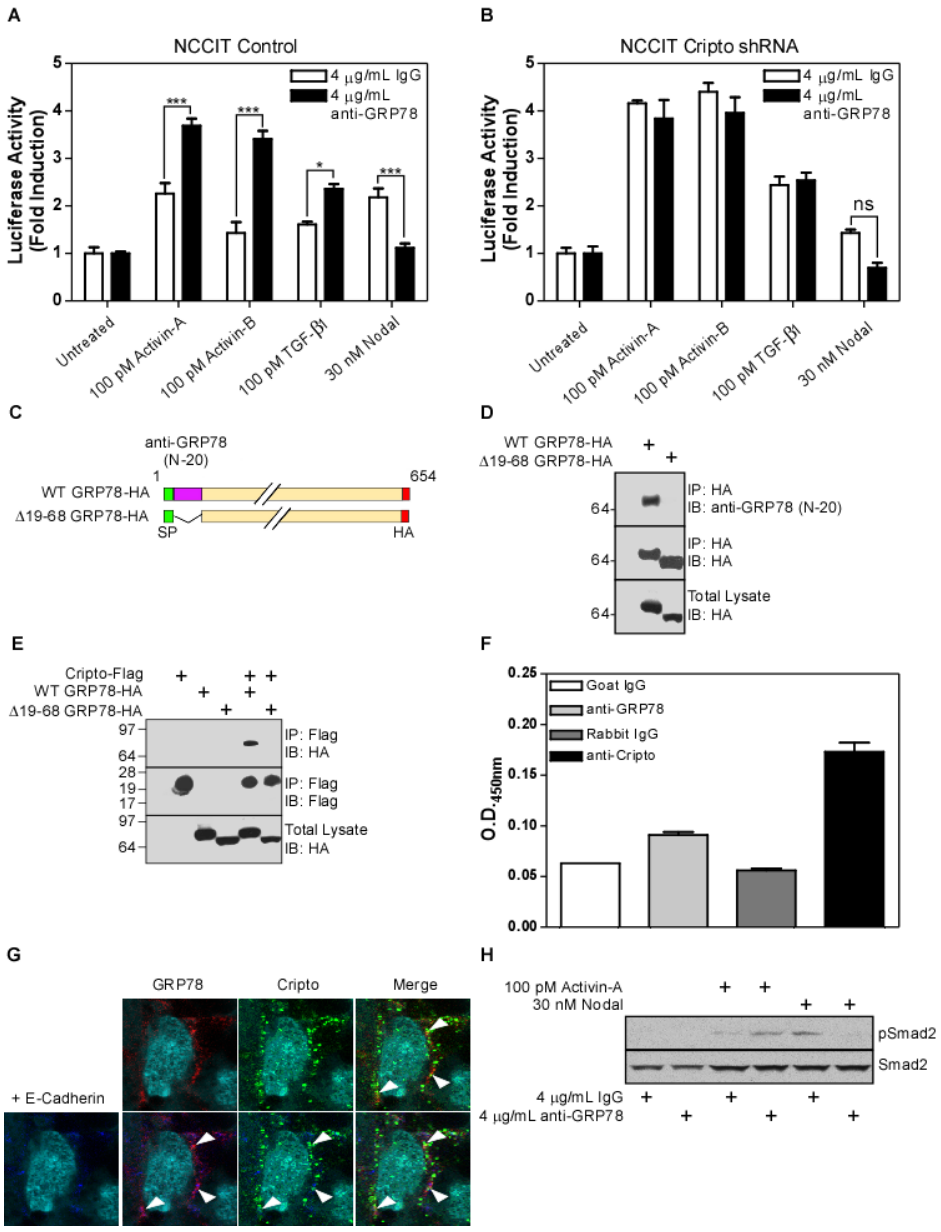

Figure 10. Antibody blockade of cell surface GRP78 inhibits Cripto signaling via TGF-β ligands in hEC and hES cells. NCCIT cells stably infected with empty vector (A) or Cripto shRNA (B) were transfected with a Smad2-responsive luciferase reporter and treated with the indicated doses of TGF-β ligands in the absence or presence of N-20 antibody as indicated. Resulting luciferase activities were normalized and are presented as fold induction over untreated samples. (C) Diagram illustrating wild type GRP78 and the Δ19-68 GRP78 construct lacking the N-20 epitope. (D, E) Lysates from 293T cells transfected with the indicated constructs were subjected to immunoprecipitation and Western blotting using anti-HA, anti-Flag and anti-GRP78 antibodies as indicated. H9 human ES cells were subjected to intact cell ELISA (F) or immunofluorescence (G) using the indicated antibodies. In (H), anti-Cripto staining is green and anti-GRP78 staining is red. (I) H9 ES cells were treated with activin-A or Nodal as indicated and resulting levels of phospho-Smad2 (pSmad2) and Smad2 were measured by Western blot using pSmad2 and Smad2 antibodies. *p<0.01; ***p<0.001.

Cripto signaling via cell surface GRP78 promotes MAPK/PI3K signaling and mitogenesis in NCCIT cells. Soluble forms of Cripto have tumor growth factor activity and activate ras/raf/ERK and PI3K/Akt pathways (Strizzi et al., 2005). Therefore, we tested whether cell surface GRP78 mediates Cripto-dependent activation of these pathways. First, we tested the effects of Cripto and/or GRP78 knockdown on Cripto-dependent phosphorylation of Akt and ERK1/2 in NCCIT cells. As shown in Figure 11A, control cells had high basal phospho-Akt levels that were unaffected by Cripto treatment. By contrast, basal phospho-Akt levels were drastically reduced in cells expressing Cripto and/or GRP78 shRNAs. Notably, Cripto treatment completely rescued Akt phosphorylation in Cripto shRNA cells in a dose-dependent manner while its ability to do so was greatly reduced when GRP78 was knocked down either alone or in combination with Cripto. Finally, Cripto-induced phosphorylation of Akt was blocked by the PI3K inhibitor, LY294002, and therefore depends on PI3K activation (Figure 11A).

We further tested the effects of Cripto and/or GRP78 knockdown on Cripto-dependent phosphorylation of ERK1/2. As shown in Figure 11B, basal ERK1/2 phosphorylation was high in control NCCIT cells and unaffected by Cripto treatment, again suggesting endogenous Cripto levels are sufficient for maximal

Cripto-dependent activation of this pathway. By contrast, basal phospho-ERK1/2 was undetectable in Cripto knockdown cells and treatment of these cells with Cripto caused pronounced phosphorylation of ERK2 (p42). This result is consistent with the previous demonstration that soluble Cripto triggers ERK2 phosphorylation in mammary epithelial cells (Kannan et al., 1997). Similar to what was observed in Cripto knockdown cells, basal phospho-ERK levels were very low in cells expressing GRP78 shRNA. However, Cripto treatment of these cells was unable to stimulate ERK phosphorylation, suggesting that GRP78 is required for Cripto-dependent activation of the MAPK pathway (Figure 11B).

Cripto tumor growth factor activity is associated with increased cellular proliferation (Strizzi et al., 2005) and we tested whether soluble Cripto promotes proliferation of NCCIT cells in a GRP78-dependent manner. As shown in Figure 11C, the basal proliferation rate of control NCCIT cells was unaffected by soluble Cripto treatment, consistent with our data showing that Cripto treatment has no effect on MAPK/PI3K signaling in these cells. By contrast, Cripto and/or GRP78 knockdown reduced NCCIT cell proliferation. Importantly, soluble Cripto treatment rescued proliferation of Cripto knockdown cells but had no effect on cells in which GRP78 was knocked down either alone or in combination with Cripto.

Next, we used the N-20 antibody to directly assess the role of cell surface GRP78 in mediating Cripto growth factor activity. Initially, we tested the ability of this antibody to compete with soluble Cripto for binding to NCCIT cells stably expressing Cripto shRNA. As shown in Figure 11D, ^{125}I-Cripto bound to these cells specifically and was displaced in a dose-dependent manner by the N-20 antibody but not by control IgG. Together with the results presented in Figure 10G, these data indicate that Cripto and the N-20 antibody directly compete for binding to the same N-terminal site on GRP78. We went on to test the ability of the N-20 antibody to block Cripto-dependent Akt phosphorylation in NCCIT cells expressing Cripto shRNA. As shown in Figure 11E, soluble Cripto-dependent Akt phosphorylation in these cells was markedly attenuated by the N-20 antibody. We further asked whether the ability of Cripto treatment to rescue proliferation in Cripto knockdown cells was GRP78 dependent. Figure 11F shows that the N-20 antibody completely blocked the pro-proliferative effect of Cripto treatment. Together, these data indicate that Cripto binding to cell surface GRP78 is required for Cripto-dependent MAPK/PI3K signaling and mitogenic effects in embryonal carcinoma cells.

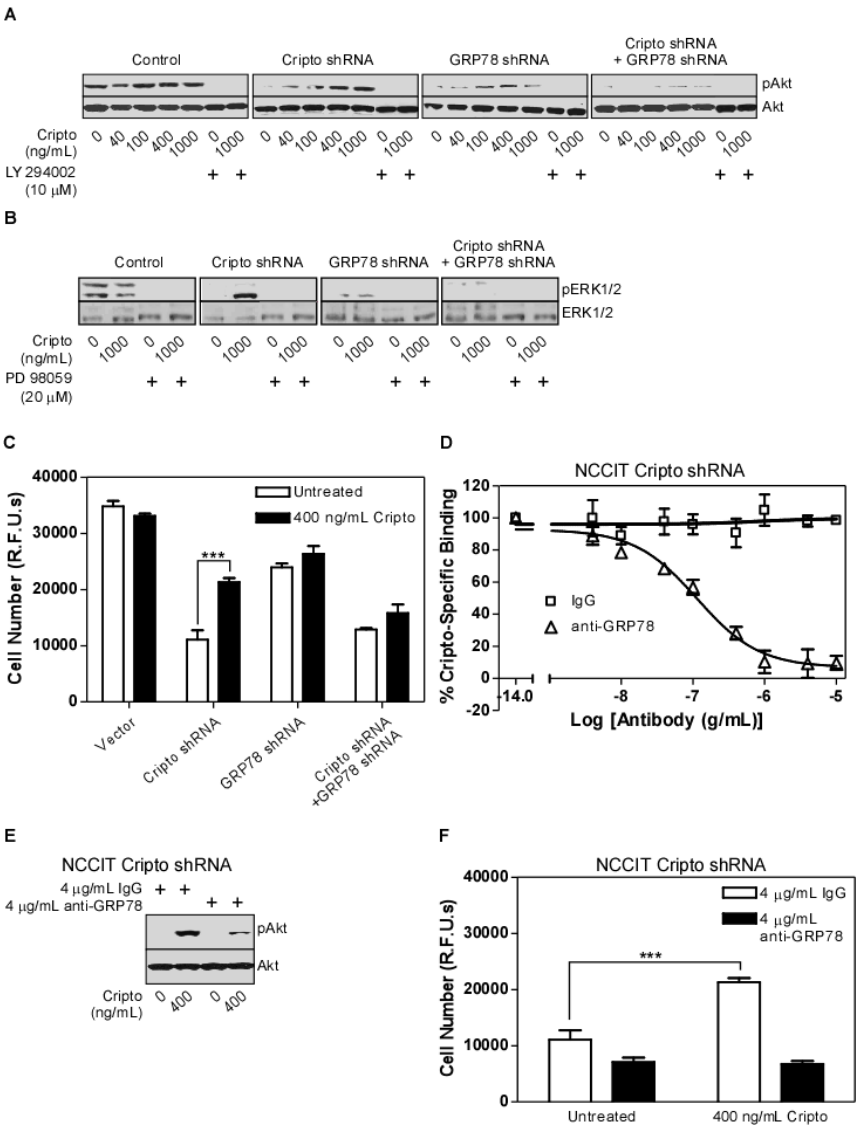

Figure 11. Cripto signaling via cell surface GRP78 promotes MAPK/PI3K signaling and mitogenesis in NCCIT cells. NCCIT cells stably expressing the indicated shRNAs were serum starved and then treated with the indicated doses of soluble Cripto and either the PI3K inhibitor (LY2940002) (A) or the MEK1/2 inhibitor (PD98059) (B) as indicated. Cell lysates were subjected to Western blotting using anti-phospho-Akt (pAkt) and Akt (A) or phospho-ERK1/2 (pERK1/2) and ERK1/2 antibodies (B) as indicated. (C) The same NCCIT cells were treated with Cripto as indicated, grown for 8 days and then proliferation was measured using the CyQuant proliferation assay kit. (D) NCCIT cells infected with Cripto shRNA were subjected to ^{125}I-Cripto binding in the presence of a range of doses of N-20 antibody or IgG control. Cripto specific binding represents the amount of ^{125}I-Cripto binding that is blocked by an excess of unlabeled soluble Cripto. NCCIT cells infected with Cripto shRNA were (E) serum-starved and then treated with the indicated dose of soluble Cripto after pretreatment with the indicated dose of IgG or anti-GRP78 (N-20) or (F) treated with soluble Cripto following pretreatment with IgG or anti-GRP78 (N-20) antibody as indicated. Cells were grown for an additional 8 days and proliferation was measured using the CyQuant proliferation assay kit. *p<0.01; ***p<0.001.

Cell surface GRP78 mediates Cripto tumor growth factor activity in human mammary epithelial cells. Cripto promotes the tumorigenic phenotype in mammary epithelial cells and is overexpressed in ~80% of human breast cancers (Strizzi et al., 2005). Therefore, we tested whether GRP78 mediates oncogenic Cripto signaling in human mammary epithelial MCF10A cells. To conduct these studies, we generated MCF10A cell clones stably infected with a control vector or a Cripto expression vector. As shown in Figure 12A, control cells had undetectable levels of Cripto expression while cells infected with the Cripto expression vector had high levels of Cripto expression as determined by Western blot. We tested whether GRP78 is present on the surface of control MCF10A cells and, as shown in Figure 12B, a fraction of GRP78 was clearly surface-exposed as measured by intact cell ELISA. Furthermore, ^{125}I-Cripto bound control MCF10A cells specifically and was displaced in a dose-dependent manner by the N-20 antibody (Figure 12C) indicating cell surface-exposed GRP78 is also capable of binding Cripto. Treatment of mammary epithelial cells with soluble Cripto activates MAPK/ERK and PI3K/Akt pathways and this has been shown to require upstream activation of c-Src (Bianco et al., 2003). Therefore, we tested if the N-20 antibody blocks Cripto-dependent c-Src activation in MCF10A cells. As shown in Figure 12D, soluble Cripto caused phosphorylation of c-Src on Tyrosine 416 in control MCF10A cells and this was blocked by

pre-incubation of the cells with N-20 antibody. Consistent with this, Cripto overexpression in MCF10A cells caused a dramatic increase in cellular proliferation that was substantially inhibited by treatment of cells with the N-20 GRP78 antibody (Figure 12E). Furthermore, as shown in Figure 12F, treatment of control MCF10A cells with soluble Cripto increased their proliferation in a manner that was completely blocked by co-treatment with the same GRP78 immunoneutralizing antibody.

Cripto causes migration and invasion of mammary epithelial cells and promotes EMT (Strizzi et al., 2005; Strizzi et al., 2004). Loss of E-Cadherin expression is a hallmark of EMT and we have tested whether cell surface GRP78 mediates Cripto-dependent downregulation of E-Cadherin in human mammary epithelial MCF10A cells. As shown in Figure 12G, E-Cadherin expression was reduced following treatment of control MCF10A cells with soluble Cripto and was undetectable in Cripto overexpressing cells. However, pretreatment of cells with the N-20 antibody reversed the Cripto-dependent decrease in E-Cadherin levels that was observed in control cells and dramatically rescued E-Cadherin expression in Cripto overexpressing cells (Figure 12G). Importantly, the rescue of E-Cadherin expression in Cripto-overexpressing cells by the N-20 antibody was almost completely blocked by co-treatment with soluble

Cripto indicating Cripto and the N-20 antibody compete functionally for binding to cell surface GRP78.

E-cadherin mediates cell-cell adhesion in epithelial cells and therefore we asked whether cell surface GRP78 mediates Cripto effects on adhesion of MCF10A cells. To test this, MCF10A control and Cripto-overexpressing cells were pretreated with the N-20 or control IgG antibodies. Cell adhesion was then analyzed after allowing these cells to adhere to tissue culture plastic for one hour. As shown in Figure 12H, the amount of cell adhesion was reduced by ~50% in Cripto overexpressing cells relative to control cells, consistent with the ability of Cripto to cause down regulation of E-Cadherin. Importantly, while the N-20 antibody had no effect on adhesion of control cells, it abrogated the Cripto-dependent decrease in cell adhesion (Figure 12H) indicating cell surface GRP78 is required for this effect. Together, these data demonstrate that cell surface GRP78 mediates the ability of Cripto to promote cellular proliferation and to decrease E-Cadherin expression and cell adhesion in human mammary epithelial cells.

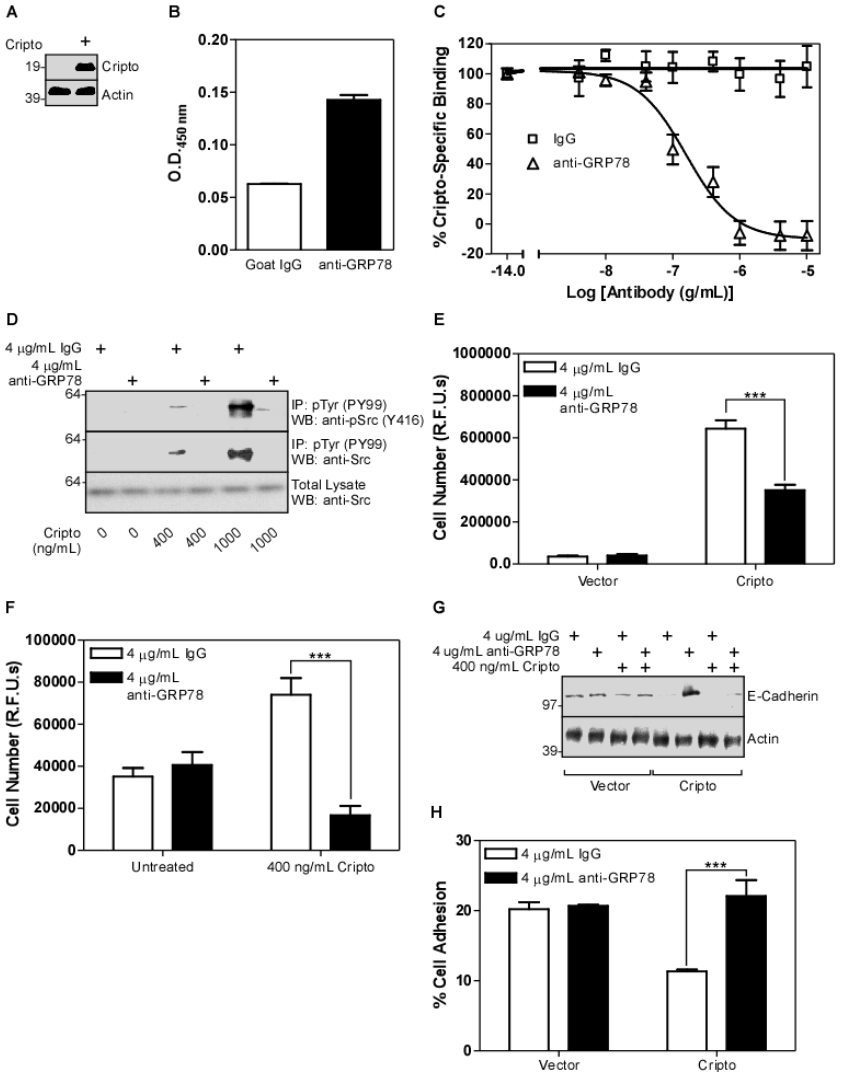

Figure 12. Cell surface GRP78 mediates Cripto tumor growth factor activity in human mammary epithelial cells. (A) Cell lysates from control or Cripto-infected MCF10A cells were analyzed by Western blot using Cripto and actin antibodies as indicated. Human mammary epithelial MCF10A cells infected with empty vector were subjected to intact cell ELISA using IgG or N-20 antibody (B) or to ^{125}I-Cripto binding in the presence of a range of doses of N-20 antibody or control IgG antibody as indicated (C). (D) MCF10A cells infected with empty vector were serum starved and then treated with the indicated doses of soluble Cripto, N-20 antibody and/or IgG as indicated. Resulting cell lysates were subjected to immunoprecipitation with anti-phospho-Tyr (pTyr) antibody and Western blotting with anti-phospho-Src (pSrc, Y416) or anti-Src antibodies as indicated. MCF10A cells infected with either empty vector or Cripto (E) or with empty vector (F) were treated with soluble Cripto, IgG and/or N-20 antibody as indicated. Cells were grown for 8 days and proliferation was measured using the CyQuant proliferation assay kit. (G) MCF10A cells infected with empty vector or Cripto were treated with soluble Cripto after pretreatment with IgG or N-20 antibody as indicated. Cell lysates were analyzed by Western blot using E-Cadherin and actin antibodies. (H) MCF10A cells infected with empty vector or Cripto were pre-treated with IgG or N-20 antibody, plated and allowed to adhere. Resulting cell adhesion was quantified using the CyQuant adhesion assay. ***$p<0.001$.

The cell surface interaction between Cripto and GRP78 facilitates pro-proliferative effects of activin-A and Nodal. We have shown here that GRP78 mediates Cripto effects on activin and Nodal signaling and therefore we tested whether Cripto/GRP78 complexes impact activin-A- and Nodal-induced effects on cellular proliferation. As shown in Figure 13A, activin-A and Nodal both increased proliferation of control NCCIT cells. Rather than acting as a pro-proliferative cytokine, activin-A had cytostatic effects on NCCIT cells with Cripto and/or GRP78 knocked down while Nodal had no effect (Figure 13A). We further tested whether treatment of NCCIT control cells with the N-20 antibody would mimic the effects of Cripto and/or GRP78 knockdown on activin-A- and Nodal-induced proliferation. Indeed, as shown in Figure 13B, the proliferative effects of activin-A and Nodal were blocked in the presence of the N-20 antibody and activin-A again acquired cytostatic properties.

Next, we tested whether Cripto and GRP78 similarly control the proliferative effects of activin-A and Nodal on MCF10A cells. As shown in Figure 13C, activin-A substantially inhibited proliferation of MCF10A control cells while Nodal had no effect, consistent with our inability to detect Cripto in these cells (Figure 13A). MCF10A cells overexpressing Cripto had an increased rate of proliferation relative to control cells and were no longer growth-inhibited by activin-A. Rather, activin-A and Nodal each increased proliferation of these cells (Figure 13C).

Importantly, treatment of Cripto-expressing MCF10A cells with the N-20 antibody blocked the pro-proliferative effects of activin-A and Nodal and caused activin-A to revert to its antiproliferative status. Therefore, the cell surface interaction between Cripto and GRP78 inhibits cytostatic effects of activin-A and, interestingly, facilitates pro-proliferative responses to both activin-A and Nodal in embryonal carcinoma and human mammary epithelial cells.

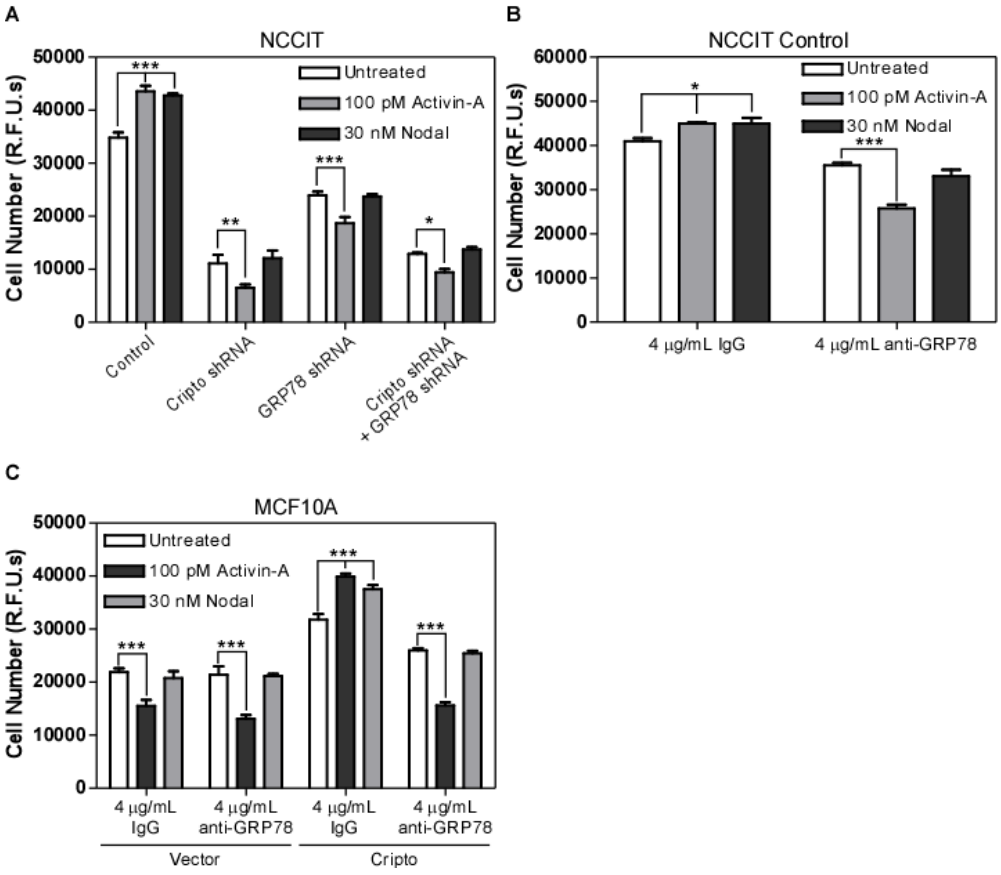

Figure 13. The cell surface interaction between Cripto and GRP78 facilitates pro-proliferative effects of activin and Nodal. NCCIT cells infected with empty vector, Cripto and/or GRP78 shRNAs (A, B) and MCF10A cells infected with empty vector or Cripto (C) were left untreated or treated with activin-A or Nodal in the absence or presence of IgG or N-20 antibody as indicated. Cells were grown for an additional 8 days and proliferation was measured using the CyQuant proliferation assay kit. *** $p<0.001$; ** $p<0.005$; * $p<0.01$.

Cripto binding to cell surface GRP78 promotes the tumorigenic phenotype. The data presented here support a model in which the cell surface Cripto/GRP78 complex acts as an oncogenic control node that promotes the tumor phenotype (Figure 14A). According to this model, Cripto and GRP78 cooperatively inhibit cytostatic Smad2/3 signaling in response to activin and TGF-β and cause activin, Nodal and TGF-β to adopt pro-proliferative effects. Concurrently, GRP78 mediates Cripto tumor growth factor activity, i.e. Cripto-dependent Src, ERK and Akt activation, increased cellular proliferation and decreased E-Cadherin expression and cell adhesion. Importantly, antibody blockade of GRP78 disrupts the cell surface Cripto/GRP78 complex and inhibits Cripto-dependent signaling (Figure 14B). The resulting inhibition of PI3K and MAPK signaling as well as the potential for increased Smad2/3 activation are likely to contribute to the tumor suppressive outcome of GRP78 immunoneutralization.

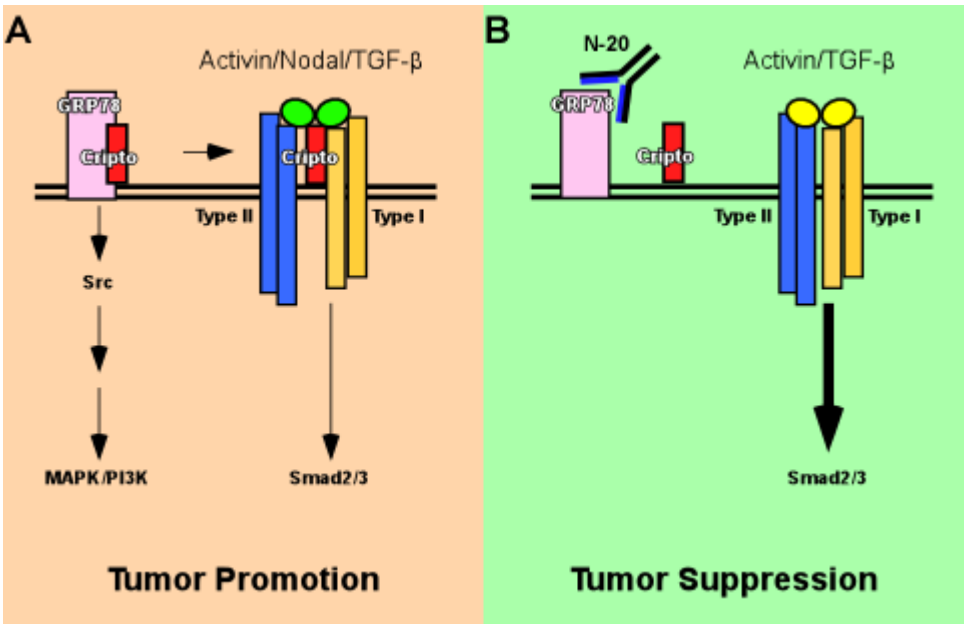

Figure 14. Cripto binding to cell surface GRP78 promotes the tumorigenic phenotype. (A) The cell surface Cripto/GRP78 complex has a pro-tumorigenic effect and a dual signaling role. Cripto binding to cell surface GRP78 leads to MAPK and PI3K signaling. Cripto binding to cell surface GRP78 also facilitates Cripto effects on signaling by activin/Nodal/TGF-β ligands leading to intermediate levels of Smad2/3 activation. The signaling effects mediated by the cell surface Cripto/GRP78 complex may increase tumor growth and metastasis. (B) Immunoneutralization of cell surface GRP78 blocks Cripto binding to surface exposed GRP78 in tumor and mammary epithelial cells and inhibits Cripto-dependent signaling via MAPK, PI3K and Smad2/3 pathways. Under these conditions, activin and TGF-β can elicit high levels of Smad2/3 signaling resulting in cytostatic responses and tumor suppression.

DISCUSSION

Independent lines of evidence have established Cripto and GRP78 as critical survival/pro-proliferation factors during normal developmental processes and cancer progression (Lee, 2007; Strizzi et al., 2005). For example, both Cripto (Strizzi et al., 2005) and GRP78 (Dong et al., 2008; Lee, 2007) increase malignancy and provide a competitive growth advantage to tumor cells by increasing tumor cell survival, proliferation and angiogenesis. In support of these overlapping biological functions, we show here that targeted disruption of the cell

surface Cripto/GRP78 complex bocks oncogenic Cripto signaling via MAPK/PI3K and Smad2/3 pathways. We further demonstrate that blocking GRP78 inhibits the ability of Cripto to promote cellular proliferation and to decrease E-Cadherin expression and cell adhesion. We draw this evidence from human embryonal carcinoma, embryonic stem and mammary epithelial cells suggesting a broad range of biological functions for the Cripto/GRP78 complex.

Although generally restricted to the lumen of the ER in normal tissues, GRP78 is localized to the cell surface of tumor cells and has been identified as a tumor-specific antigen in primary human breast and prostate cancer samples (Arap et al., 2004; Jakobsen et al., 2007). In addition, GRP78 antibodies were found in the serum of prostate cancer patients and shown to serve as a biomarker of increased cancer aggressiveness (Arap et al., 2004). Cell surface GRP78 has also been validated as a tumor-selective target since chimeric peptides composed of GRP78 binding motifs fused to an apoptosis-inducing sequence inhibited tumor growth in mouse models of prostate and breast cancer (Arap et al., 2004; Liu et al., 2007). Importantly, cell surface GRP78 appears to have an oncogenic function since it mediated activation of MAPK and PI3K pathways after binding α2-macroglobulin in 1-LN prostate carcinoma cells resulting in pro-proliferative and anti-apoptotic behavior (Misra et al., 2006). T-Cadherin binding to cell surface GRP78 was also shown to have an

essential role in mediating survival signal transduction via Akt in endothelial cells (Philippova et al., 2008). In addition, tumorigenesis and Akt activation resulting from Pten loss in prostate epithelium is blocked by prostate-specific disruption of GRP78 expression (Fu et al., 2008), a finding that is consistent with the ability of cell surface GRP78 to initiate Akt signaling.

Our discovery that GRP78 mediates Cripto modulation of multiple TGF-β superfamily members suggests that surface-exposed GRP78 may serve as an anchor or scaffold that allows Cripto to adopt a conformation or an orientation necessary for its functional interaction with these ligands and their receptors. By contrast, our demonstration that GRP78 mediates Cripto-dependent activation of c-Src and MAPK/PI3K pathways resembles previous findings suggesting GRP78 can operate as a cell surface signaling receptor (Misra et al., 2006; Philippova et al., 2008). Alternatively, cell surface GRP78 may indirectly couple Cripto to c-Src, MAPK and PI3K activation as a critical component of a larger protein complex, possibly involving other proteins that have been implicated in Cripto signaling such as glypican-1 (Bianco et al., 2003), ErbB4 (Bianco et al., 1999) and/or Tomoregulin-1 (Harms and Chang, 2003). We previously reported that the CFC domain of Cripto binds GRP78 (Shani et al., 2008) and we have shown here that the extreme N-terminus of GRP78 is required for Cripto binding. Interestingly, T-Cadherin (Philippova et al., 2008) and

α2-macroglobulin (Gonzalez-Gronow et al., 2006) also bind cell surface-exposed GRP78 near its N-terminus suggesting these proteins and Cripto may share a common mode of activating GRP78 receptor function. It will be important for future work to identify whether other circulating growth factors regulate Cripto's ability to bind to and signal through GRP78 via the MAPK/PI3K and Smad2/3 pathways. While the exact mechanism of GRP78-mediated Cripto signaling remains to be elucidated, our data demonstrating a physical and functional dependence of oncogenic Cripto signaling on cell surface GRP78 is novel and provides significant insight into how disrupting this tumor-sellective, cell surface protein complex may abrogate the tumor phenotype.

Our results show that shRNA knockdown of Cripto and/or GRP78 or antibody blockade of GRP78 in NCCIT cells enhances activin-A, activin-B and TGF-β1 signaling while inhibiting Nodal signaling. These data represent the first demonstration that endogenously expressed Cripto inhibits activin signaling and confirm our previous demonstration that endogenous Cripto blocks signaling by TGF-β1 (Gray et al., 2006). Knockdown of Cripto and GRP78 together affected the signaling of these TGF-β ligands to a greater extent than knockdown of either protein alone indicating Cripto and GRP78 function cooperatively. In support of this, a GRP78 blocking antibody that disrupts Cripto/GRP78 binding abolished Cripto-dependent effects

on signaling by activin/Nodal/TGF-β ligands. Since Cripto-dependent Nodal signaling has essential functions during early embryogenesis (Shen, 2007), our data point to a novel and critical role for cell surface GRP78 during development. In support of this, we have also made the exciting observation that GRP78 is present at the surface of human ES cells where it co-localizes with Cripto. Furthermore, we have shown that an immunoneutralizing antibody that targets the Cripto binding site on GRP78 has opposing effects on Nodal and activin-A signaling similar to what was observed following Cripto knockdown in NCCIT cells. It is instructive to consider these results in light of recent evidence suggesting that aberrantly activated developmental programs can give rise to tumor growth and metastasis in the adult. Therefore, while the cell surface Cripto/GRP78 complex may be required for proper development, our data suggest that the function of this protein complex is dysreglated during tumorigenesis.

Our data indicate that GRP78 is a necessary mediator of Cripto tumor growth factor activity since knockdown or antibody blockade of cell surface GRP78 prevented Cripto-dependent activation of PI3K/Akt and MAPK/ERK pathways. Cripto has been reported to activate these pathways via c-Src (Bianco et al., 2003) and we have shown here that Cripto-dependent c-Src activation in human mammary epithelial MCF10A cells is blocked by GRP78 immunoneutralization. Furthermore, our results show that shRNA knockdown or antibody

blockade of cell surface GRP78 prevents Cripto from increasing cellular proliferation of NCCIT and MCF10A cells. E-Cadherin mediates calcium-dependent cell-cell adhesion and its loss is associated with invasive, metastatic cancer (Peinado et al., 2007). Importantly, we have shown that blocking cell surface GRP78 prevents Cripto-induced loss of E-Cadherin expression and cellular adhesion. Thus, our data support a necessary role for GRP78 in mediating Cripto's effects on proliferation, migration, invasion and EMT.

TGF-β ligands that activate Smad2/3 signaling can inhibit or promote tumorigenesis depending on the cellular context and on whether tumor cells have become refractory to the antiproliferative effects of the Smad2/3 pathway (Rahimi and Leof, 2007). We have shown here that activin-A has opposing effects on cellular proliferation depending on the presence or absence of cell surface Cripto/GRP78 complexes. Activin-A had pro-proliferative effects on NCCIT cells and MCF10A cells in which cell surface Cripto/GRP78 complexes were intact but had antiproliferative effects when these complexes were disrupted by knockdown or immunoneutralization. Notably, this finding resembles our previous demonstration that co-expression of Cripto and GRP78 caused TGF-β1 to switch from having cytostatic effects to having pro-proliferative effects on PC3 prostate carcinoma cells (Shani et al., 2008). Nodal also increased proliferation in cells that expressed intact Cripto/GRP78 complexes but, unlike activin-A and TGF-β1,

Nodal had no effect on the proliferation of cells in which Cripto/GRP78 complexes were disrupted. This difference between activin-A and TGF-β1 as opposed to Nodal likely reflects the fact that Cripto is required for Nodal signaling but not for activin-A or TGF-β1 signaling. Thus, our results indicate that Cripto and GRP78 can cooperate to promote tumor growth in part by facilitating mitogenic effects of Nodal and causing activin-A and TGF-β1 to switch from being cytostatic to pro-proliferative in nature.

In summary, we have shown that Cripto binding to cell surface GRP78 is required for Cripto signaling in human tumor, ES and mammary epithelial cells. Cripto and GRP78 have each been independently identified as cell surface tumor-selective targets *in vivo* and we have shown here that they also co-localize at the surface of hESCs. Our findings indicate that the cell surface Cripto/GRP78 complex has important developmental roles and that targeted disruption of this complex represents a novel approach for abrogating tumor growth and metastasis.

Chapter 2, in full, contains text and data in preparation for publication (with Panopoulos AD, Shani G, Booker EC, Belmonte JC, Vale WW, Gray PC). The disseratation author is the primary investigator and author of this report.

CONCLUSION

The work presented here represents several significant advances in our understanding of how Cripto regulates the MAPK, PI3K and Smad2/3 signaling pathways to promote cellular effects that are characteristic of the tumor phenotype. Specifically, we have demonstrated that Cripto modifies ligand-dependent receptor assembly by activin and Nodal to confer a reduced level of Smad2/3 activity. Furthermore, we have identified several ALK4 ECD point mutations that confer Cripto-specific binding and which can target several of Cripto functions. We have also demonstrated that GRP78 is necessary for Cripto's ability to activate the MAPK/PI3K pathways and to modulate the Smad2/3 pathway. The fact that the Cripto/GRP78 complex is selectively found on the surface of tumor and embryonic stem cells suggests that targeting this interaction in these contexts may lead to selective interference of Cripto-mediated signaling functions. Importantly, targeted disruption of this complex may facilitate more directed, less systemically toxic cancer therapies. Furthermore, these same approaches may drive directed differentiation of embryonic stem cells toward lineages that Cripto has been shown to block (e.g. neuroectoderm), facilitating cell-replacement therapies. Finally, it will be important for future studies to investigate the exact mechanism by which GRP78 mediates Cripto signaling function. These studies may provide insight into how

specific targeting of this interaction may selectively target the specific functions of Cripto-mediated signaling. Additionally, *in vivo* studies will support our *in vitro* data demonstrating that cell surface GRP78 mediates oncogenic Cripto-dependent signaling.

REFERENCES

Adewumi, O., Aflatoonian, B., Ahrlund-Richter, L., Amit, M., Andrews, P.W., Beighton, G., Bello, P.A., Benvenisty, N., Berry, L.S., Bevan, S., Blum, B., Brooking, J., Chen, K.G., Choo, A.B., Churchill, G.A., Corbel, M., Damjanov, I., Draper, J.S., Dvorak, P., Emanuelsson, K., Fleck, R.A., Ford, A., Gertow, K., Gertsenstein, M., Gokhale, P.J., Hamilton, R.S., Hampl, A., Healy, L.E., Hovatta, O., Hyllner, J., Imreh, M.P., Itskovitz-Eldor, J., Jackson, J., Johnson, J.L., Jones, M., Kee, K., King, B.L., Knowles, B.B., Lako, M., Lebrin, F., Mallon, B.S., Manning, D., Mayshar, Y., McKay, R.D., Michalska, A.E., Mikkola, M., Mileikovsky, M., Minger, S.L., Moore, H.D., Mummery, C.L., Nagy, A., Nakatsuji, N., O'Brien, C.M., Oh, S.K., Olsson, C., Otonkoski, T., Park, K.Y., Passier, R., Patel, H., Patel, M., Pedersen, R., Pera, M.F., Piekarczyk, M.S., Pera, R.A., Reubinoff, B.E., Robins, A.J., Rossant, J., Rugg-Gunn, P., Schulz, T.C., Semb, H., Sherrer, E.S., Siemen, H., Stacey, G.N., Stojkovic, M., Suemori, H., Szatkiewicz, J., Turetsky, T., Tuuri, T., van den Brink, S., Vintersten, K., Vuoristo, S., Ward, D., Weaver, T.A., Young, L.A. and Zhang, W. (2007) Characterization of human embryonic stem cell lines by the International Stem Cell Initiative. *Nat Biotechnol*, **25**, 803-816.

Adkins, H.B., Bianco, C., Schiffer, S.G., Rayhorn, P., Zafari, M., Cheung, A.E., Orozco, O., Olson, D., De Luca, A., Chen, L.L., Miatkowski, K., Benjamin, C., Normanno, N., Williams, K.P., Jarpe, M., LePage, D., Salomon, D. and Sanicola, M. (2003) Antibody blockade of the Cripto CFC domain suppresses tumor cell growth in vivo. *J Clin Invest*, **112**, 575-587.

Allendorph, G.P., Vale, W.W. and Choe, S. (2006) Structure of the ternary signaling complex of a TGF-beta superfamily member. *Proc Natl Acad Sci U S A*, **103**, 7643-7648.

Arap, M.A., Lahdenranta, J., Mintz, P.J., Hajitou, A., Sarkis, A.S., Arap, W. and Pasqualini, R. (2004) Cell surface expression of the stress response chaperone GRP78 enables tumor targeting by circulating ligands. *Cancer Cell*, **6**, 275-284.

Attisano, L., Wrana, J.L., Cheifetz, S. and Massague, J. (1992) Novel activin receptors: distinct genes and alternative mRNA splicing

generate a repertoire of serine/threonine kinase receptors. *Cell*, **68**, 97-108.

Bianco, C., Adkins, H.B., Wechselberger, C., Seno, M., Normanno, N., De Luca, A., Sun, Y., Khan, N., Kenney, N., Ebert, A., Williams, K.P., Sanicola, M. and Salomon, D.S. (2002) Cripto-1 activates nodal- and ALK4-dependent and -independent signaling pathways in mammary epithelial Cells. *Mol Cell Biol*, **22**, 2586-2597.

Bianco, C., Kannan, S., De Santis, M., Seno, M., Tang, C.K., Martinez-Lacaci, I., Kim, N., Wallace-Jones, B., Lippman, M.E., Ebert, A.D., Wechselberger, C. and Salomon, D.S. (1999) Cripto-1 indirectly stimulates the tyrosine phosphorylation of erb B-4 through a novel receptor. *J Biol Chem*, **274**, 8624-8629.

Bianco, C., Strizzi, L., Rehman, A., Normanno, N., Wechselberger, C., Sun, Y., Khan, N., Hirota, M., Adkins, H., Williams, K., Margolis, R.U., Sanicola, M. and Salomon, D.S. (2003) A Nodal- and ALK4-independent signaling pathway activated by Cripto-1 through Glypican-1 and c-Src. *Cancer Res*, **63**, 1192-1197.

Carcamo, J., Weis, F.M., Ventura, F., Wieser, R., Wrana, J.L., Attisano, L. and Massague, J. (1994) Type I receptors specify growth-inhibitory and transcriptional responses to transforming growth factor beta and activin. *Mol Cell Biol*, **14**, 3810-3821.

Chen, C., Ware, S.M., Sato, A., Houston-Hawkins, D.E., Habas, R., Matzuk, M.M., Shen, M.M. and Brown, C.W. (2006) The Vg1-related protein Gdf3 acts in a Nodal signaling pathway in the pre-gastrulation mouse embryo. *Development*, **133**, 319-329.

Chen, R.H., Ebner, R. and Derynck, R. (1993) Inactivation of the type II receptor reveals two receptor pathways for the diverse TGF-beta activities. *Science*, **260**, 1335-1338.

Cheng, S.K., Olale, F., Bennett, J.T., Brivanlou, A.H. and Schier, A.F. (2003) EGF-CFC proteins are essential coreceptors for the TGF-beta signals Vg1 and GDF1. *Genes Dev*, **17**, 31-36.

Cheng, S.K., Olale, F., Brivanlou, A.H. and Schier, A.F. (2004) Lefty Blocks a Subset of TGFbeta Signals by Antagonizing EGF-CFC Coreceptors. *PLoS Biol*, **2**, E30.

Davidson, D.J., Haskell, C., Majest, S., Kherzai, A., Egan, D.A., Walter, K.A., Schneider, A., Gubbins, E.F., Solomon, L., Chen, Z., Lesniewski, R. and Henkin, J. (2005) Kringle 5 of human plasminogen induces apoptosis of endothelial and tumor cells through surface-expressed glucose-regulated protein 78. *Cancer Res*, **65**, 4663-4672.

Debnath, J., Muthuswamy, S.K. and Brugge, J.S. (2003) Morphogenesis and oncogenesis of MCF-10A mammary epithelial acini grown in three-dimensional basement membrane cultures. *Methods*, **30**, 256-268.

Dong, D., Ni, M., Li, J., Xiong, S., Ye, W., Virrey, J.J., Mao, C., Ye, R., Wang, M., Pen, L., Dubeau, L., Groshen, S., Hofman, F.M. and Lee, A.S. (2008) Critical role of the stress chaperone GRP78/BiP in tumor proliferation, survival, and tumor angiogenesis in transgene-induced mammary tumor development. *Cancer Res*, **68**, 498-505.

Fu, Y., Wey, S., Wang, M., Ye, R., Liao, C.P., Roy-Burman, P. and Lee, A.S. (2008) Pten null prostate tumorigenesis and AKT activation are blocked by targeted knockout of ER chaperone GRP78/BiP in prostate epithelium. *Proc Natl Acad Sci U S A*.

Gonzalez-Gronow, M., Cuchacovich, M., Llanos, C., Urzua, C., Gawdi, G. and Pizzo, S.V. (2006) Prostate cancer cell proliferation in vitro is modulated by antibodies against glucose-regulated protein 78 isolated from patient serum. *Cancer Res*, **66**, 11424-11431.

Gray, P.C., Greenwald, J., Blount, A.L., Kunitake, K.S., Donaldson, C.J., Choe, S. and Vale, W. (2000) Identification of a Binding Site on the Type II Activin Receptor for Activin and Inhibin. *J. Biol. Chem.*, **275**, 3206-3212.

Gray, P.C., Harrison, C.A. and Vale, W. (2003) Cripto forms a complex with activin and type II activin receptors and can block activin signaling. *Proc Natl Acad Sci U S A*, **100**, 5193-5198.

Gray, P.C., Shani, G., Aung, K., Kelber, J. and Vale, W. (2006) Cripto binds transforming growth factor beta (TGF-beta) and inhibits TGF-beta signaling. *Mol Cell Biol*, **26**, 9268-9278.

Greenwald, J., Vega, M.E., Allendorph, G.P., Fischer, W.H., Vale, W. and Choe, S. (2004) A flexible activin explains the membrane-dependent cooperative assembly of TGF-beta family receptors. *Mol Cell*, **15**, 485-489.

Harms, P.W. and Chang, C. (2003) Tomoregulin-1 (TMEFF1) inhibits nodal signaling through direct binding to the nodal coreceptor Cripto. *Genes Dev*, **17**, 2624-2629.

Harrison, C.A., Gray, P.C., Fischer, W.H., Donaldson, C., Choe, S. and Vale, W. (2004) An activin mutant with disrupted ALK4 binding blocks signaling via type II receptors. *J Biol Chem*, **279**, 28036-28044.

Harrison, C.A., Gray, P.C., Koerber, S.C., Fischer, W. and Vale, W. (2003) Identification of a functional binding site for activin on the type I receptor ALK4. *J Biol Chem*, **278**, 21129-21135.

Harrison, C.A., Gray, P.C., Vale, W.W. and Robertson, D.M. (2005) Antagonists of activin signaling: mechanisms and potential biological applications. *Trends Endocrinol Metab*, **16**, 73-78.

Hemmati-Brivanlou, A. and Melton, D.A. (1992) A truncated activin receptor inhibits mesoderm induction and formation of axial structures in Xenopus embryos. *Nature*, **359**, 609-614.

Jakobsen, C.G., Rasmussen, N., Laenkholm, A.V. and Ditzel, H.J. (2007) Phage display derived human monoclonal antibodies isolated by binding to the surface of live primary breast cancer cells recognize GRP78. *Cancer Res*, **67**, 9507-9517.

Kannan, S., De Santis, M., Lohmeyer, M., Riese, D.J., 2nd, Smith, G.H., Hynes, N., Seno, M., Brandt, R., Bianco, C., Persico, G., Kenney, N., Normanno, N., Martinez-Lacaci, I., Ciardiello, F., Stern, D.F., Gullick, W.J. and Salomon, D.S. (1997) Cripto enhances the tyrosine phosphorylation of Shc and activates mitogen-activated protein kinase (MAPK) in mammary epithelial cells. *J Biol Chem*, **272**, 3330-3335.

Kelber, J.A., Shani, G., Booker, E.C., Vale, W.W. and Gray, P.C. (2008) Cripto is a noncompetitive activin antagonist that forms analogous signaling complexes with activin and nodal. *J Biol Chem*, **283**, 4490-4500.

Lee, A.S. (2007) GRP78 induction in cancer: therapeutic and prognostic implications. *Cancer Res*, **67**, 3496-3499.

Liu, Y., Steiniger, S.C., Kim, Y., Kaufmann, G.F., Felding-Habermann, B. and Janda, K.D. (2007) Mechanistic Studies of a Peptidic GRP78 Ligand for Cancer Cell-Specific Drug Delivery. *Mol Pharm*.

Massague, J. and Gomis, R.R. (2006) The logic of TGFbeta signaling. *FEBS Lett*, **580**, 2811-2820.

Mathews, L.S. and Vale, W.W. (1991) Expression cloning of an activin receptor, a predicted transmembrane serine kinase. *Cell*, **65**, 973-982.

Mathews, L.S., Vale, W.W. and Kintner, C.R. (1992) Cloning of a second type of activin receptor and functional characterization in *Xenopus* embryos. *Science*, **255**, 1702-1705.

McDowell, N. and Gurdon, J.B. (1999) Activin as a morphogen in Xenopus mesoderm induction. *Semin Cell Dev Biol*, **10**, 311-317.

Minchiotti, G. (2005) Nodal-dependant Cripto signaling in ES cells: from stem cells to tumor biology. *Oncogene*, **24**, 5668-5675.

Minchiotti, G., Manco, G., Parisi, S., Lago, C.T., Rosa, F. and Persico, M.G. (2001) Structure-function analysis of the EGF-CFC family member Cripto identifies residues essential for nodal signalling. *Development*, **128**, 4501-4510.

Misra, U.K., Deedwania, R. and Pizzo, S.V. (2006) Activation and cross-talk between Akt, NF-kappaB, and unfolded protein response signaling in 1-LN prostate cancer cells consequent to ligation of cell surface-associated GRP78. *J Biol Chem*, **281**, 13694-13707.

Misra, U.K., Gonzalez-Gronow, M., Gawdi, G., Wang, F. and Pizzo, S.V. (2004) A novel receptor function for the heat shock protein Grp78: silencing of Grp78 gene expression attenuates alpha2M*-induced signalling. *Cell Signal*, **16**, 929-938.

Miyoshi, H., Blomer, U., Takahashi, M., Gage, F.H. and Verma, I.M. (1998) Development of a self-inactivating lentivirus vector. *J Virol*, **72**, 8150-8157.

Nicolas, F.J. and Hill, C.S. (2003) Attenuation of the TGF-beta-Smad signaling pathway in pancreatic tumor cells confers resistance to TGF-beta-induced growth arrest. *Oncogene*, **22**, 3698-3711.

Pardali, K. and Moustakas, A. (2007) Actions of TGF-beta as tumor suppressor and pro-metastatic factor in human cancer. *Biochim Biophys Acta*, **1775**, 21-62.

Parish, C.L., Parisi, S., Persico, M.G., Arenas, E. and Minchiotti, G. (2005) Cripto as a target for improving embryonic stem cell-based therapy in Parkinson's disease. *Stem Cells*, **23**, 471-476.

Parisi, S., D'Andrea, D., Lago, C.T., Adamson, E.D., Persico, M.G. and Minchiotti, G. (2003) Nodal-dependent Cripto signaling promotes cardiomyogenesis and redirects the neural fate of embryonic stem cells. *J Cell Biol*, **163**, 303-314.

Peinado, H., Olmeda, D. and Cano, A. (2007) Snail, Zeb and bHLH factors in tumour progression: an alliance against the epithelial phenotype? *Nat Rev Cancer*, **7**, 415-428.

Philippova, M., Ivanov, D., Joshi, M.B., Kyriakakis, E., Rupp, K., Afonyushkin, T., Bochkov, V., Erne, P. and Resink, T.J. (2008) Identification of proteins associating with GPI-anchored T-cadherin on the surface of vascular endothelial cells: the role for Grp78/BiP in T-cadherin-dependent cell survival. *Mol Cell Biol*.

Piek, E., Westermark, U., Kastemar, M., Heldin, C.H., van Zoelen, E.J., Nister, M. and Ten Dijke, P. (1999) Expression of transforming-growth-factor (TGF)-beta receptors and Smad proteins in glioblastoma cell lines with distinct responses to TGF- beta1. *Int J Cancer*, **80**, 756-763.

Piepenburg, O., Grimmer, D., Williams, P.H. and Smith, J.C. (2004) Activin redux: specification of mesodermal pattern in Xenopus by graded concentrations of endogenous activin B. *Development*, **131**, 4977-4986.

Postovit, L.M., Margaryan, N.V., Seftor, E.A., Kirschmann, D.A., Lipavsky, A., Wheaton, W.W., Abbott, D.E., Seftor, R.E. and Hendrix, M.J. (2008) Human embryonic stem cell microenvironment suppresses the tumorigenic phenotype of aggressive cancer cells. *Proc Natl Acad Sci U S A*, **105**, 4329-4334.

Rahimi, R.A. and Leof, E.B. (2007) TGF-beta signaling: a tale of two responses. *J Cell Biochem*, **102**, 593-608.

Ramis, J.M., Collart, C. and Smith, J.C. (2007) Xnrs and Activin Regulate Distinct Genes during Xenopus Development: Activin Regulates Cell Division. *PLoS ONE*, **2**, e213.

Reissmann, E., Jornvall, H., Blokzijl, A., Andersson, O., Chang, C., Minchiotti, G., Persico, M.G., Ibanez, C.F. and Brivanlou, A.H. (2001) The orphan receptor ALK7 and the Activin receptor ALK4 mediate signaling by Nodal proteins during vertebrate development. *Genes Dev*, **15**, 2010-2022.

Schier, A.F. (2003) Nodal signaling in vertebrate development. *Annu Rev Cell Dev Biol*, **19**, 589-621.

Schmierer, B. and Hill, C.S. (2007) TGFbeta-SMAD signal transduction: molecular specificity and functional flexibility. *Nat Rev Mol Cell Biol*, **8**, 970-982.

Shani, G., Fischer, W.H., Justice, N.J., Kelber, J.A., Vale, W. and Gray, P.C. (2008) GRP78 and Cripto form a complex at the cell surface and collaborate to inhibit transforming growth factor beta signaling and enhance cell growth. *Mol Cell Biol*, **28**, 666-677.

Shen, M.M. (2003) Decrypting the role of Cripto in tumorigenesis. *J Clin Invest*, **112**, 500-502.

Shen, M.M. (2007) Nodal signaling: developmental roles and regulation. *Development*, **134**, 1023-1034.

Shen, M.M. and Schier, A.F. (2000) The EGF-CFC gene family in vertebrate development. *Trends Genet*, **16**, 303-309.

Shi, Y. and Massague, J. (2003) Mechanisms of TGF-beta signaling from cell membrane to the nucleus. *Cell*, **113**, 685-700.

Shukla, A., Ho, Y., Liu, X., Ryscavage, A. and Glick, A.B. (2008) Cripto-1 alters keratinocyte differentiation via blockade of transforming growth factor-beta1 signaling: role in skin carcinogenesis. *Mol Cancer Res*, **6**, 509-516.

Singer, O., Marr, R.A., Rockenstein, E., Crews, L., Coufal, N.G., Gage, F.H., Verma, I.M. and Masliah, E. (2005) Targeting BACE1 with siRNAs ameliorates Alzheimer disease neuropathology in a transgenic model. *Nat Neurosci*, **8**, 1343-1349.

Strizzi, L., Bianco, C., Normanno, N. and Salomon, D. (2005) Cripto-1: a multifunctional modulator during embryogenesis and oncogenesis. *Oncogene*, **24**, 5731-5741.

Strizzi, L., Bianco, C., Normanno, N., Seno, M., Wechselberger, C., Wallace-Jones, B., Khan, N.I., Hirota, M., Sun, Y., Sanicola, M. and Salomon, D.S. (2004) Epithelial mesenchymal transition is

a characteristic of hyperplasias and tumors in mammary gland from MMTV-Cripto-1 transgenic mice. *J Cell Physiol*, **201**, 266-276.

Tendijke, P., Yamashita, H., Ichijo, H., Franzen, P., Laiho, M., Miyazono, K. and Heldin, C.H. (1994) Characterization of Type-I receptors for transforming growth factor-beta and activin. *Science*, **264**, 101-104.

Thompson, T.B., Woodruff, T.K. and Jardetzky, T.S. (2003) Structures of an ActRIIB:activin A complex reveal a novel binding mode for TGF-beta ligand:receptor interactions. *Embo J*, **22**, 1555-1566.

Topczewska, J.M., Postovit, L.M., Margaryan, N.V., Sam, A., Hess, A.R., Wheaton, W.W., Nickoloff, B.J., Topczewski, J. and Hendrix, M.J. (2006) Embryonic and tumorigenic pathways converge via Nodal signaling: role in melanoma aggressiveness. *Nat Med*, **12**, 925-932.

Tsuchida, K., Vaughan, J.M., Wiater, E.M., Gaddy-Kurten, D. and Vale, W.W. (1995) Inactivation of activin-dependent transcription by kinase-deficient activin receptors. *Endocrinology*, **136**, 5493-5503.

Vaughan, J.M. and Vale, W.W. (1993) Alpha 2-macroglobulin is a binding protein of inhibin and activin. *Endocrinology*, **132**, 2038-2050.

Wechselberger, C., Strizzi, L., Kenney, N., Hirota, M., Sun, Y., Ebert, A., Orozco, O., Bianco, C., Khan, N.I., Wallace-Jones, B., Normanno, N., Adkins, H., Sanicola, M. and Salomon, D.S. (2005) Human Cripto-1 overexpression in the mouse mammary gland results in the development of hyperplasia and adenocarcinoma. *Oncogene*.

Xing, P.X., Hu, X.F., Pietersz, G.A., Hosick, H.L. and McKenzie, I.F. (2004) Cripto: a novel target for antibody-based cancer immunotherapy. *Cancer Res*, **64**, 4018-4023.

Xu, C., Liguori, G., Adamson, E.D. and Persico, M.G. (1998) Specific arrest of cardiogenesis in cultured embryonic stem cells lacking Cripto-1. *Dev Biol*, **196**, 237-247.

Yan, Y.T., Liu, J.J., Luo, Y., E, C., Haltiwanger, R.S., Abate-Shen, C. and Shen, M.M. (2002) Dual roles of Cripto as a ligand and coreceptor in the nodal signaling pathway. *Mol Cell Biol*, **22**, 4439-4449.

Yeo, C. and Whitman, M. (2001) Nodal signals to Smads through Cripto-dependent and Cripto-independent mechanisms. *Mol Cell*, **7**, 949-957.

Yu, J. and Thomson, J.A. (2008) Pluripotent stem cell lines. *Genes Dev*, **22**, 1987-1997.